UNIVERSIDADE DE SÃO PAULO

INSTITUTO DE FÍSICA
CAIXA POSTAL 20516
01498 - SÃO PAULO - SP
BRASIL

PUBLICAÇÕES

IFUSP/P-696

COMPARISONS BETWEEN SENIORITY, QUASI-PARTICLE AND SHELL MODEL CALCULATIONS: APPLICATION TO THE ODD Ni ISOTOPES AND ODD N=82 ISOTONES

L. Losano
Departamento de Física, Universidade Federal da Paraíba, João Pessoa, Brasil

H. Dias
Instituto de Física, Universidade de São Paulo

F. Krmpotić
Departamento de Física, Universidad Nacional de La Plata, La Plata, Argentina

B.H. Wildenthal
Departament of Physics, University of New Mexico, Albuquerque, USA

Março/1988

ABSTRACT

A detailed study of shell model correlations induced into the BCS approximation by the number projection method and by blocking effect, has been carried out. The low seniority shell model was used as the frame of reference to investigate the mixing of one and three quasi particle states in odd-mass Ni isotopes and in odd-mass N=82 isotones. We discuss the results obtained for the energy spectra and electromagnetic decay properties. Effects of seniority - five configurations on the low lying states has also been studied through the comparison of low seniority shell model results with those which arise from the full shell model calculations.

1. INTRODUCTION

Because of the dimensions of the problem, the only versions of the shell model applicable for medium and heavy nuclei with open shells are those based on the quasiparticle BCS approximations. One of such approaches, widely used in the description of single-close nuclei, is the Tamm-Dancoff approximation (TDA). The spurious effects due to the non-conservation of the number of particles in the quasiparticle method can be removed, although only partially, following the procedure of Kuo et al[1]. A complete elimination of the spurious states can be achieved only by performing the number projection[2-6]. However, in this improved formalism, called projected BCS approximation (PBCS), we are losing a great deal of the physical transparency, which is one of the most proeminent advantages of the simple-minded BCS method.

Furthermore, the PBCS approach do not take into account the fact that pairing correlations may be different for different nuclear states. Namely, in the PBCS formalism the diffuseness of the Fermi energy surface for all the states is determined in the BCS ground state. We know, nevertheless, that the Fermi surface becomes more and more sharp as the number of quasiparticles increases and that pairing correlations vanish totally in highly excited states. To improve on the BCS and PBCS methods one should perform a new energy-minimization

procedure for each state, with respect to its total energy. The importance of this effect, usually called blocking effect, in relation with odd mass nuclei, has already been pointed out and discussed qualitatively a long time ago by Nilsson[7]. The BCS formalism with blocking included (BBCS) retains most of the simplicity of the BCS method, although it clearly still contains the spurious effects related with the particle-number non-conservation.

Several comparative studies between the BCS and PBCS methods in relation with the properties of odd mass nuclei have been done[3-6]. However, no such study was performed, so far, for the blocking effect within the BCS formalism even though the BBCS method is much more transparent than the PBCS formalism. The relative importances of the blocking effect and the number projection, i.e., a comparison between the BBCS and PBCS methods, is also an opened question. Such comparison was done only recently[8] for the three valence particle nuclei ($^{135}_{53}I_{82}$). In that work we compared differents BCS approximations within the model space of one and three quasiparticles (1QP + 3QP) and the exact calculations. From that comparison it was suggested that the blocking effect and number projection may play an important role in the description of low-lying states in odd mass nuclei. For nuclei with more than three valence particle such comparison has never been done.

The main aim of the present work is to study the shell model correlation induced into the BCS approximation by

the number projection method and by the blocking effect. We will limit our attention to low-lying states of odd mass nuclei which will be described within 1QP + 3 QP subspace. In order to stablish the frame of reference for the foregoing correlations we will also describe the same nuclei within the exact shell model using the same residual interaction and the same set of parameters. To our knowledge no such study has been performed so far. As a matter of fact, the results for two different shell model calculations will be presented. In the first case, only configuration states with seniority (ν) smaller than three are considered. This approach, which will be called low seniority shell model (LSSM), is the exact limit for all BCS approximations within the subspace of 1QP + 3QP. In the second case, the complete shell model (CSM) calculation is performed and from comparison with the LSSM results we will be able to infer to which extent the configurations with ν = 5 participate in building up the structure of low-lying state. A comparison with experimental data is not our aim, but this will be subject of a forthcoming paper, in which the method explained here will be used[9].

This paper is organized in the following way: we devote Section 2 to the description of the different BCS formalisms. Shell model formalism is plantifully discussed in the literature[10,11] and will not be described here. In Section 3, we give details of the numerical calculations. In subsection 4.1 we investigate, through the comparison between the CSM and LSSM calculations, the effects of configurations with ν = 5 on the

structure of the low-lying states. In subsection 4.2 the influence of configurations with $\nu = 3$ and 1 and with a number of quasi-particles, N_{qp}, higher than five is studied by comparison the LSSM and PBCS calculations. In subsection 4.3 we discuss the correlations induced by the BBCS and PBCS approximation. Finally some general conclusions are drawn out in section 5.

2. FORMALISM

2.1. EVALUATION OF THE MATRIX ELEMENTS

In order to calculate the matrix elements of the shell model hamiltonian,

$$H = \sum_{\alpha} \varepsilon_{\alpha} a_{\alpha}^{\dagger} a_{\alpha} + \frac{1}{4} \sum_{\alpha\beta\gamma\delta} \langle \alpha\beta | v | \gamma\delta \rangle \, a_{\alpha}^{\dagger} a_{\beta}^{\dagger} a_{\delta} a_{\gamma} \tag{2.1}$$

and on the one-body operators

$$T_{\lambda\mu} = \sum_{\alpha\beta} \langle \alpha | T_{\lambda\mu} | \beta \rangle a_{\alpha}^{\dagger} a_{\beta} \tag{2.2}$$

where $a_{\alpha}^{\dagger}(a_{\alpha})$ are particle creation (destruction) operators, $\alpha \equiv (j_a, m_a)$ and $\bar{\alpha} = (-)^{j_a - m_a}(j_a, -m_a)$, we introduce a z-dependent canonical transformation[8]

$$\begin{aligned} d_{\alpha} &= \sqrt{\sigma_a}(u_a a_{\alpha} - z v_a a_{\bar{\alpha}}^{\dagger}) \quad , \\ d_{\alpha}^{*} &= \sqrt{\sigma_a}(u_a^{*} a_{\alpha}^{\dagger} - z v_a^{*} a_{\bar{\alpha}}) \quad , \end{aligned} \tag{2.3}$$

with

$$\sigma_a = (u_a u_a^{*} + z^2 v_a v_a^{*})^{-1} \quad . \tag{2.4}$$

Here, (u_a, v_a) and (u_a^{*}, v_a^{*}) are the BCS parameters in the

ket-states and bra-states, respectively, and the symbol * on the creation operator d^*_α stands for the hermitian conjugation (†) plus the transformation $(u_a, v_a) \leftrightarrow (u^*_a, v^*_a)$. It is easy to see that

$$\{d^*_\alpha, d_\beta\} = \delta_{\alpha\beta} \quad , \tag{2.5}$$

and

$$d_\alpha |0;z\rangle = \langle 0;z| d^*_\alpha = 0 \quad , \tag{2.6}$$

where

$$|0;z\rangle = \prod_{\alpha>0} (u_a + z v_a a^\dagger_\alpha a^\dagger_{\bar\alpha}) |0\rangle \quad , \tag{2.7}$$

and $|0\rangle$ represents the particle vacua.

By means of the inverse transformation

$$a^\dagger_\alpha = \sqrt{\sigma_a}\ (u_a d^*_\alpha + z v_a d_{\bar\alpha}) \quad , \tag{2.8a}$$

$$a_\alpha = \sqrt{\sigma_a}\ (u^*_a d_\alpha + z\, v_a d^*_{\bar\alpha}) \quad , \tag{2.8b}$$

the hamiltonian reads

$$H = H_{00} + H_{11} + H_{20} + H^*_{20} + H_{22} + H_{31} + H^*_{31} + H_{40} + H^*_{40} \ , \tag{2.9}$$

with

$$H_{00} = \sum_a \hat a^2 \sigma_a z^2 \left[v_a v^*_a (\epsilon_a - \tfrac{1}{2}\mu_a) - \tfrac{1}{2} u_a v^*_a \Delta_a \right] \quad , \tag{2.10a}$$

$$H_{11} = -\sum_a \hat a \sigma_a \Big[(u_a u^*_a - z^2 v_a v^*_a)(\epsilon_a - \mu_a) + z^2 (u_a v^*_a \Delta_a + u^*_a v_a \Delta^*_a) \Big] \overline{D}_{00}(aa) \quad , \tag{2.10b}$$

$$H_{20} = \sum_a \hat a \sigma_a \left[z\, u_a v_a (\epsilon_a - \mu_a) - \tfrac{1}{2} (u^2_a \Delta_a - z^2 v^2_a \Delta^*_a) \right] D^*_{00}(aa) \ , \tag{2.10c}$$

$$H_{22} = \frac{1}{8} \sum_{\substack{abcd \\ JM}} (\sigma_a \sigma_b \sigma_c \sigma_d)^{1/2} \Big[(u_a u_b u^*_c u^*_d + z^4 v_a v_b v^*_c v^*_d) g_J(abcd) + 4 z^2 u_a v_b u^*_c u^*_d f_J(abcd) \Big] D^*_{JM}(ab)\, D_{JM}(cd) \quad , \tag{2.10d}$$

$$H_{31} = -\frac{1}{4} \sum_{\substack{abcd \\ JM}} (\sigma_a \sigma_b \sigma_c \sigma_d)^{1/2} z\, g_J(bacd) (u_a u_b u^*_c v_d - z^2 v_a v_b v^*_c v_d) \times (-)^{J+M} D^*_{J-M}(ba)\, \overline{D}_{JM}(cd) \quad , \tag{2.10e}$$

$$H_{40} = -\frac{1}{8} \sum_{\substack{abcd \\ JM}} (\sigma_a \sigma_b \sigma_c \sigma_d)^{1/2} z^2 g_J(bacd) u_a u_b v_c v_d \times (-)^{J+M} D^*_{J-M}(ba)\, D^*_{JM}(cd) \quad , \tag{2.10f}$$

where the operators $\bar{D}_{JM}(ab)$ and $D^*_{JM}(ab)$ are defined as

$$\bar{D}_{JM}(ab) = \sum_{m_\alpha m_\beta} (j_a m_a j_b m_b | JM)\, d^*_\alpha d_{\bar{\alpha}} \qquad (2.11a)$$

and

$$D^*_{JM}(ab) \equiv [D_{JM}(ab)]^* = \sum_{m_\alpha m_\beta} (j_a m_a j_b m_b | JM)\, d^*_\beta d^*_\alpha \quad . \qquad (2.11b)$$

The gap parameters Δ_a and the chemical potentials μ_a are given by

$$\Delta_a = -\frac{1}{4} z \hat{a}^{-1} \sum_c \hat{c} g_0(aacc)\, \sigma_c v_c u^*_c \quad , \qquad (2.12)$$

and

$$\mu_a = -\frac{1}{2} z \hat{a}^{-1} \sum_c \hat{c} f_0(aacc)\, \sigma_c v_c v^*_c \quad . \qquad (2.13)$$

The quantities $f_J(abcd)$ and $g_J(abcd)$ are antisymmetrized matrix elements of the interaction[3] and $\hat{a} \equiv (2j_a+1)^{1/2}$.

In the same way the transition operator (2.2) takes the form

$$T_{\lambda\mu} = -\hat{\lambda}^{-1} \sum_{ab} (\sigma_a \sigma_b)^{1/2} \langle a \| T_\lambda \| b \rangle \left\{ \left[(-)^x u_a u^*_b - z^2 v^*_a v_b \right] \bar{D}_{\lambda\mu}(ab) \right.$$
$$+ \frac{1}{2} z \left[u_a v_b + (-)^x v_a u_b \right] D^*_{\lambda\mu}(ab) + \frac{1}{2} z \left[v^*_a v^*_b + (-)^x v^*_a v^*_b \right] D_{\lambda\bar{\mu}}(ab) \Big\}$$
$$+ \delta_{\lambda 0} \delta_{\mu 0} \sum_a \hat{a} v_a v^*_a \sigma_a \langle a \| T_\lambda \| a \rangle \quad , \qquad (2.14)$$

where $x = 0$ and 1 for electric and magnetic moments, respectively.

The generating wave fucntions[3] are rewritten as

$$|\alpha; z\rangle = \sqrt{\sigma_a}\, z d^*_\alpha |0, z\rangle \quad , \qquad (2.15a)$$

for a one-quasiparticle state (1QP),

$$|(ab)JM; z\rangle = (\sigma_a \sigma_b)^{1/2}$$
$$\times \left[z^2 D^*_{JM}(ab) - \delta_{J0} \delta_{ab} \hat{a} z (u_a v^*_a z^2 - v_a u^*_a) \right] |0, z\rangle \quad , \qquad (2.15b)$$

for a two-quasiparticle state (2QP) and

$$|[(ab)J, c]IM; z\rangle = (\sigma_a \sigma_b \sigma_c)^{1/2}$$
$$\times \left(z^3 \sum_{Mm_\gamma} (JMj_c m_\gamma | IM)\, d^*_\gamma D^*_{JM}(ab) - z^2 H(abJc, I) d^*_{IM} \right) |0; z\rangle \quad , \qquad (2.15c)$$

for a three-quasiparticle state (3QP). Here

$$H(abJc; I) = \delta_{J0} \delta_{ab} \delta_{cI} \hat{a} (u_a v^*_a z^2 - v_a u^*_a)$$
$$- \hat{J} \hat{I}^{-1} \delta_J(ab; cI) (u_c v^*_c z^2 - v_c u^*_c) \quad , \qquad (2.16)$$

and

$$\delta_J(ab,cd) = \delta_{ac}\delta_{bd} - (-)^{J+j_a+j_b}\delta_{ad}\delta_{bc} \quad . \qquad (2.17)$$

Utilizing the anti-commutation relation (2.5), the matrix elements of the operators (2.1) and (2.2) are easily calculated[12].

It should be noted that our formalism for blocking is much simpler than the one introduced by Allaart and Van Gunsteren[5] as their quasiparticle transformation is not canonical.

The results for BCS, BBCS and PBCS methods are obtained from the above mentioned formula when the following conditions are imposed:

$$u_a^* = u_a \quad , \quad v_a^* = v_a \quad \text{(PBCS)} \quad ,$$

$$z = 1 \quad \text{(BBCS)} \quad ,$$

$$u_a^* = u_a \quad , \quad v_a^* = v_a \quad \text{and} \quad z = 1 \quad \text{(BCS)} \quad .$$

2.2. RESIDUAL INTERACTION

In the next subsection, we shall utilize an interaction for which the gap equations, discussed below, are very similar to those of the pairing force, viz, the surface delta interaction (SDI)[13]. In this way, the calculation of the pairing parameters, u_a and v_a, within the formalisms which include the blocking

effect will ve greatly simplified.

The SDI is of the form

$$V(1,2) = -4\pi G\,\delta(\Omega_{12})\,\delta(r_1-R)\,\delta(r_2-R) \qquad (2.18)$$

where G is the coupling strenght, Ω_{12} the angular coordinate between the interacting particles 1 and 2, and R is the nuclear radius. The corresponding pair scattering matrix elements are

$$g_J(abcd) = G\hat{a}\hat{b}\hat{c}\hat{d}\,(-)^{\ell_a+\ell_c+j_b+j_d}\,i^{\ell_c+\ell_d+\ell_a+\ell_b}$$

$$\times \begin{pmatrix} J_a & J_b & J \\ \frac{1}{2} & -\frac{1}{2} & 0 \end{pmatrix} \begin{pmatrix} J_c & J_d & J \\ \frac{1}{2} & -\frac{1}{2} & 0 \end{pmatrix} \left[1 + (-)^{\ell_c+\ell_d+J}\right] \qquad (2.19)$$

In solving the gap equations one needs the matrix elements

$$g_0(aabb) = -2G\hat{a}\hat{b} \quad , \qquad (2.20a)$$

and

$$f_0(aabb) = -G\hat{a}\hat{b} \quad . \qquad (2.20b)$$

The corresponding matrix elements for the pairing force are

$$g_0(aabb) = -2G\hat{a}\hat{b} \quad , \qquad (2.21a)$$

and

$$f_0(aabb) = -2G\delta_{ab} \quad . \tag{2.21b}$$

2.3. THE GAP EQUATIONS

In order to establish the gap equations for the state $|\eta\rangle$, which may contain zero, one,... etc. quasiparticles, we always start from the variational problem

$$\delta\langle\eta|H(\lambda)|\eta\rangle = 0, \tag{2.22a}$$

$$\langle\eta|N|\eta\rangle = n_0, \tag{2.22b}$$

where

$$H(\lambda) = H - \lambda N, \tag{2.23}$$

n_0 is the number of valence particles, λ is the chemical potential and N is the particle number operator.

Within the BCS and PBCS formalism all the pairing properties are defined in the BCS vacuum ($|\eta\rangle \equiv |0;z=1\rangle$) and from expressions (2.22) one obtains the standard gap equations for the parameters u_s and v_s

$$2u_s v_s(\varepsilon_s - \mu_s - \lambda) - (u_s^2 - v_s^2)\Delta_s = 0 \quad , \tag{2.24a}$$

$$\sum_r \hat{r}^2 v_r^2 = n_0 \quad . \tag{2.24b}$$

When the blocking effect is considered the state $|\eta\rangle$ is no more the BCS vacuum but the blocked state. Below we discuss the corresponding gap equations.

In the case of 1QP, the gap equations, for the quasiparticle in the state ($|\eta\rangle = |\alpha;z=1\rangle$) $|\alpha\rangle$, reads

$$\left[2u_s v_s(\varepsilon_s - \mu_s - \lambda) - \Delta_s(u_s^2 - v_s^2)\right](1 - 2\hat{s}^{-2}\delta_{sa})$$

$$- \frac{(u_s^2 - v_s^2)u_a v_a}{2\hat{a}\hat{s}} g_0(aass) + \frac{2u_s v_s u_a^2 v_a^2}{\hat{a}\hat{s}} f_0(aass) = 0 \quad , \tag{2.25a}$$

$$\sum_r (\hat{r}^2 - 2\delta_{ar}) v_r^2 = n_o - 1 \quad . \tag{2.25b}$$

Note that for $j_s = j_a = \frac{1}{2}$ these equations does not allow us to determine the values of the parameters $u_{\frac{1}{2}}$ and $v_{\frac{1}{2}}$. This fact, however, is irrelevant because when the blocked particle is in the state $j_a = \frac{1}{2}$ the quantities $u_{\frac{1}{2}}$ and $v_{\frac{1}{2}}$ do not appear explicitly in the calculation. We can see that from (2.15a) which, for $j_a = \frac{1}{2}$, reads

$$|\tfrac{1}{2}m;z\rangle = z\, a^\dagger_{\frac{1}{2}m} \prod_{\substack{\alpha>0 \\ j_a\neq\frac{1}{2}, m_a\neq\frac{1}{2}}} (u_a + z_a v_a a^\dagger_\alpha a^\dagger_{\bar{\alpha}})|0\rangle \tag{2.26}$$

Before going to the 3QP case it is convenient to discuss the gap equations for two quasiparticles. If the blocked states are $|\alpha\rangle$ and $|\beta\rangle$, ($|\eta\rangle = |(ab)JM;z=1\rangle$) equations

(2.22), leads to

$$\left[2u_s v_s(\varepsilon_s - \mu_s - \lambda) - \Delta_s(u_s^2 - v_s^2)\right]\left[1 - \frac{2}{\hat{s}^2}(\delta_{sa} + \delta_{sb})\right] -$$

$$- \frac{(u_s^2 - v_s^2)}{2}\left[\frac{u_a v_a}{\hat{a}\hat{s}} g_0(aass) + \frac{u_b v_b}{\hat{b}\hat{s}} g_0(bbss)\right] +$$

$$+ u_s v_s\left[\frac{(u_a^2 - v_a^2)}{\hat{a}\hat{s}} f_0(aass) + \frac{(u_b^2 - v_b^2)}{\hat{b}\hat{s}} f_0(bbss)\right] +$$

$$+ \frac{u_s v_s}{(1+\delta_{ab})\hat{s}^2}\left[(u_b^2 - v_b^2)\delta_{sa} + (u_a^2 - v_a^2)\delta_{sb}\right]\left[g_J(abab) + f_J(abab)\right] -$$

$$- \frac{(u_s^2 - v_s^2)}{(1+\delta_{ab})\hat{s}^2} f_J(abba)(-)^{j_a+j_b+J}(u_b v_b \delta_{sa} + u_a v_a \delta_{sb}) = 0, \quad (2.27a)$$

$$\sum_r \left[\hat{r}^2 - 2(\delta_{ra} + \delta_{rb})\right] v_r^2 = n_0 - 2 \quad (2.27b)$$

The number of gap equations which should be solved is equal to the dimension of the configuration space for two quasiparticles (all allowed values of j_a, j_b and J). In the work of Akkermans et al[6] the criterium adopted, in order to simplify the problem was to neglect the quasiparticle residual interaction (which means to ignore the last two terms in (2.27a)). In this way the number of gap equations is drastically reduced as it now depends only on the possible single particle states j_a and j_b.

In the present work a similar approximation is done, but following a different criterium. At first it should be noted that for the gap equations (2.24) nad (2.25) are the same for SDI and the pairing force, except for the self energy term μ_s, which is equal to

$$\mu_s = G v_s^2 \quad (2.28a)$$

for the pairing force, and to

$$\mu_s = \frac{G}{2}\sum_r \hat{r}^2 v_r^2 \quad (2.28b)$$

for SDI. Having in view, furthermore, that for the pairing force the expression (2.27a) reduces to

$$\left[2u_s v_s(\varepsilon_s - \mu_s - \lambda) - (u_s^2 - v_s^2)(\Delta_s - G u_a v_a - G u_b v_b)\right] \times$$

$$\times \left[1 - 2\hat{s}^{-2}(\delta_{as} + \delta_{bs})\right] - 2G u_s v_s(u_s^2 - v_s^2)\delta_{J0}\delta_{as}\delta_{bs} = 0, \quad (2.30)$$

it seems reasonable to work with this last equation in place of using (2.27a). It should be noted, however, that we are still in trouble as the equation (2.30) is identically satisfied for any value of $u_{\frac{1}{2}}$ and $v_{\frac{1}{2}}$, when $J = 0$. Then, in this case, we are obliged to use the unblocked pairing parameters. There is, in principle, no problem in solving the gap equations for

the remaining seniority zero-two quasiparticle states. However, bearing in mind that the seniority zero states are not orthogonal to each other with blocking effect taken into account[7], what makes the BBCS formalism complicated, we decide to use for all seniority zero-two quasiparticle states the unblocked pairing parameters. With this procedure the basis is now orthogonal and the spurious states are removed following the same technique used in BCS approach. It is worth mentioning that, in general, the number of configuration with seniority zero is very small in comparison with the number of states with seniority two.

For the 3QP states we adopted the same approximations discussed before for the 2QP states. Therefore, the gap equations for three quasiparticles blocked in the states $|\alpha\rangle$, $|\beta\rangle$ and $|\gamma\rangle$, ($|\eta\rangle = |[(ab)J,c]IM;z=1\rangle$), leads to

$$\left\{2u_s v_s(\epsilon_s - \mu_s - \lambda) - (u_s^2 - v_s^2)\left[\Delta_s - G(u_a v_a + u_b v_b + u_c v_c)\right]\right\} \times$$

$$\times \left(1 - \frac{2}{\hat{s}^2}(\delta_{sa} + \delta_{sb} + \delta_{sc})\right) = 0 \qquad (2.31a)$$

$$\sum_s \left[\hat{s}^2 - 2(\delta_{sa} + \delta_{sb} + \delta_{sc})\right] v_s^2 = n_0 - 3 \quad . \qquad (2.31b)$$

3. Numeric calculations

We restrict ourselves to single closed-shell nuclei where only an odd number of nucleons in the open subshells are considered. For our study two examples are considered: the Ni (Z = 28) isotopes and N = 82 isotones. In the first case we investigated the nuclei with 3, 5, 7 and 9 neutrons occupying the subshells $2p_{3/2}$, $1f_{5/2}$ and $2p_{1/2}$. Therefore only negative parity states will be considered. In the second case we focus our attention to the nuclei with 3, 5, 7, 9 and 11 protons occupying the subshells $2d_{5/2}$, $1g_{7/2}$, $3s_{1/2}$ and $2d_{3/2}$. We calculated the structure of the low lying states (level schemes, eigenvectors, electromagnetic moments and transition rates) using different approaches: CSM, LSSM, BCS, BBCS and PBCS which are explained in sections 1 and 2.

In Tables 1 and 2 are presented the sizes of configuration spaces for Z = 28 isotopes and N = 82 isotones, respectively. The dimensions for all three BCS approximations and for all nuclei are equal to the numbers shown in the second columns of these tables. For further discussion it is convenient to introduce here the label N_{qp} which specifies the number of quasiparticles. Thus the difference in the number of configurations between BCS approach and the LSSM comes from the configurations with $v \leq 3$ and $N_{qp} \geq 5$. It is clear that the maximum value of N_{qp} is equal to the number of valence particles or holes.

For the N = 82 isotones we do not consider the orbital $1h_{11/2}$ as its inclusion leaves the dimension of the problem (for

CSM and LSSM) beyond the possibility of using our computational techniques. It is evident that in such a situation the utilization of approximations is essential.

For all five approximations (CSM, LSSM, BCS, BBCS and PBCS) the diagonalization procedure was carried out with the following set of parameters:

The single particle energies $\varepsilon(\ell j)$ for all Ni isotopes were extracted from experimental results for ^{57}Ni nucleus with the result 0., 0.76 and 1.08 MeV for the orbitals $p_{3/2}$, $f_{5/2}$ and $p_{1/2}$ respectively. For all odd N = 82 isotones the single particle energies were taken to be 0.0, 0.80, 2.62 and 2.68 MeV for the orbitals $g_{7/2}$, $d_{5/2}$, $d_{3/2}$ and $s_{1/2}$, respectively, as given in ref. 14.

For the residual interaction between the valence particles we used the surface delta interaction (SDI) with strengths

G = 0.48 MeV (Ni isotopes),

G = 0.20 MeV (N = 82 isotones),

which follows from the estimate of Kisslinger-Sorensen[15].

The energy spectra fo Ni isotopes are shown in Figs. 1-4 and the wave functions of a few low-lying states in ^{61}Ni and ^{63}Ni are listed in Table 3. The seniority structure of these states is presented in Tables 4 and 5.

In Figs. 5-9 are exhibited the energy spectra of N = 82 isotones from ^{135}I to ^{143}Pm, while the comparison of the wave functions obtained within different BCS approximations is

performed in Table 6. The seniority composition of the ^{137}Cs wavefunctions is presented in Table 7.

The calculations of the magnetic dipole moments, μ, and the B(M1) values were performed with the following gyromagnetic ratios:

1) $g_\ell = 0$ and $g_s^{eff} = 0.7\, g_s^{free}$ for Ni isotopes,

2) $g_\ell = 1$ and $g_s^{eff} = 0.4\, g_s^{free}$ for N = 82 isotones.

The electric quadrupole moments, Q, and the B(E2) values were evaluated with the following effective electric charges:

1) $e_n^{eff} = 1.7e$ for Ni isotopes[16], and

2) $e_p^{eff} = 2e$ for N = 82 isotones.

The results for the electromagnetic properties of Ni and N = 82 nuclei are presented in Figs. 10-13 and Figs. 14-16, respectively.

4. DISCUSSION

4.1 Effects of configurations with $\nu = 5$ on the low-lying states

In order to inquire on the way in which the configurations with $\nu = 5$ participate in establishing the structure of the low-lying states we study here the deviations of the results obtained within the LSSM with respect to those which arise from the CSM.

Firstly, we study the Ni isotopes and limit our analysis to nuclei with A=61 and 63. This is due to the fact that within the single-particle subspace considered in the present work the states in A = 59 and 65 niquel isotopes are build up only on configurations with $\nu = 1$ and 3.

From Figs. 2 and 3 one can see that the LSSM energy spectra are less compressed than the CSM ones. However, the number of states up to an excitation energy of 3 MeV obtained with these two models are not very different; within de LSSM there are 29 and 28 states for ^{61}Ni and ^{63}Ni, respectively, while the corresponding numbers within the CSM are 37 and 35.

In Tables 4 and 5 are displayed the seniority structure and the mean values of the seniority $\bar{\nu}$ for several low-lying states in ^{61}Ni and ^{63}Ni, respectively. In both approximations only the levels $1/2^-_1$, $3/2^-_1$ and $5/2^-_1$ are dominantely $\nu = 1$ sates. The remaining levels mostly contain the $\nu = 3$ configurations. As expected the values of $\bar{\nu}$ increase with excitation energy. It should also be noted that for a given

total angular momentum J the mean seniority of the state J_n is always smaller than that of the state J_{n+1} and that the influence of configurations with $\nu = 5$ commence to be pronounced for levels with $n = 3$.

We discuss below the electromagnetic properties of: i) the states with $\bar{\nu} \approx 1$, i.e., the levels $1/2^-_1$, $3/2^-_1$ and $5/2^-_1$ (with a fraction of $\nu = 5$ configurations smaller than 1%); ii) the first excited state for every one spin with $\bar{\nu} \approx 3$, i.e., the states $7/2^-_1$, $9/2^-_1$, $1/2^-_2$, $3/2^-_2$ and $5/2^-_2$ (with admixtures of $\nu = 5$ configurations between 1% and 11%); and iii) a few selected levels ($7/2^-_2$, $3/2^-_3$ and $5/2^-_3$) which are second excited states with $\bar{\nu} \approx 3$ (with the fraction of $\nu = 5$ configurations varying from 8% to 24%).

The results for the dipole magnetic and quadrupole electric moments are presented, as a function of the mass number, in Figs. 10 and 11, respectively. As one would anticipate the LSSM results practically agree with the CSM calculations for all three levels with $\bar{\nu} \approx 1$. For the second group of states, i.e., the lowest states with $\bar{\nu} \approx 3$, the differences between the LSSM and the CSM results are significant. The only exception is the value of the magnetic moment of the $1/2^-_2$ state. The differences between the two calculations of the electromagnetic moments are still more accentuated for levels which belong to the third group of states.

The B(M1) and B(E2) values for Ni isotopes, displayed in Figs. 12 and 13, respectively, always have as final state one of the levels $1/2^-_1$, $3/2^-_1$ or $5/2^-_1$. One immediately sees that when the transition is initiated in one of the levels $1/2^-_1$, $3/2^-_1$, $5/2^-_1$, $7/2^-_1$, $9/2^-_1$, $1/2^-_2$ and $3/2^-_2$, which contain relatively small

proportion of configurations with $\nu = 5$, the LSSM and the CSM yield quite similar results for the electromagnetic transitions. Moreover, the differences between both calculations are of little significance a) for the B(M1) values for which the initial states are $7/2_1^-$ and $5/2_2^-$, and b) for the B(E2) values for which the initial states are $7/2_2^-$, $3/2_3^-$ and $5/2_3^-$. When one of the levels $7/2_2^-$, $3/2_3^-$ or $5/2_3^-$ is involved in the transition process the deviations of the LSSM results with respect to the CSM ones are quite important.

In the following part of this section we will perform the comparison between the LSSM and CSM descriptions of the ^{137}Cs nucleus. Computational limitations prevent us to extend this analysis to the N = 82 isotones with more than five valence protons.

From the results shown in Fig. 6 one observes that up to 1.4 MeV in excitation energy the level scheme calculated within the LSSM is quite satisfactory when compared with the corresponding CSM spectrum. Both spectra exhibit the same number of states, the energy differences are very small ($\lesssim$120 keV) and except for the inversion of the $11/2_2^+$ and $5/2_3^+$ states, the ordering of the levels is also the same. For the states compresed in the energy interval between 1.4 and 1.6 MeV, the energy differences are relatively small, but the ordering of the levels is different and the density of states is slightly smaller within the LSSM. Above 1.6 MeV in excitation energy the influence of $\nu = 5$ configurations is quite pronounced and, as a consequence,

the level density significantly diminishes when the configuration space is truncated.

In Table 7 are shown the seniority compositions and the mean seniorities for levels with excitation energy lower than 1.6 MeV. Only the first two levels in the ^{137}Cs nucleus are dominantly seniority one states,while for all remaining levels $\bar{\nu} \approx 3$. The fraction of $\nu = 5$ configurations is smaller than 6% for states which lie below 1.4MeV, between 6 and 10% for levels with excitation energy between 1.4 and 1.6 MeV, and in most of the cases larger than 10%, and going up to 50%, for states which are above 1.6 MeV in excitation energy.

The analysis of electromagnetic properties is performed for i) the states with $\bar{\nu} \approx 1$, i.e., the levels $5/2_1^+$ and $7/2_1^+$; ii) the first excited states for each spin with $\bar{\nu} \approx 3$, i.e., the levels $1/2_1^+$, $3/2_1^+$, $9/2_1^+$, $11/2_1^+$, $13/2_1^+$, $15/2_1^+$, $5/2_2^+$ and $7/2_2^+$; and iii) the state $3/2_2^+$ due to the fact that for heavier isotones it turns out to be the lowest $\bar{\nu} \approx 3$ state with spin and parity $3/2^+$.

In Fig. 14 are compared the magnetic dipole moments for the levels $1/2_1^+$, $3/2_1^+$, $5/2_1^+$, $7/2_1^+$, $9/2_1^+$, $11/2_1^+$, $13/2_1^+$, $15/2_1^+$, $3/2_2^+$, $5/2_2^+$ and $7/2_2^+$, as well as the B(M1) values for the transitions $9/2_1^+ \longrightarrow 11/2_1^+$ and $13/2_1^+ \longrightarrow 11/2_1^+$. Except for the last transitions the LSSM and the CSM lead to almost identical results for all these observables. We do not present here the results for the remaining M1 transitions which take place among the above mentioned states. It is due to the fact that, as a

consequence of the ℓ-forbiddeness, all they are very weak (smaller than 10^{-3}W.u.) and therefore the tensor M1 operater $[Y_2 \otimes \vec{\sigma}]_1$, not considered in the present work, plays an important role.

From the results, shown in Fig. 15 for the electric quadrupole moments of the low-lying states in the ^{137}Cs nucleus, we see that the effect of configurations with $\nu = 5$ on these observables is negligible small for the levels $7/2^+_1$, $9/2^+_1$, $11/2^+_1$ and $3/2^+_2$. The differences between the LSSM and CSM results for the remaining six states, although relatively small, are significant. It is worthwhile to notice that in the case of the $5/2^+_1$ and $5/2^+_2$ levels these differences arise both 1) from the rearrengement of the $\nu = 1$ and $\nu = 3$ amplitudes in the corresponding wave functions, induced by the $\nu = 5$ configurations (see Table 7) and 2) from the destructive interference between the $\nu = 1$ and $\nu = 3$ contributions on the quadrupole moments $Q(5/2^+_1)$ and $Q(5/2^+_2)$.

The results for the B(E2) values, exhibited in Fig.16, clearly demonstrate that relatively small admixture of $\nu = 5$ configurations, in the low-lying states, affect the magnitudes of the $5/2^+_1 \longrightarrow 7/2^+_1$, $5/2^+_2 \longrightarrow 7/2^+_1$, $9/2^+_1 \longrightarrow 11/2^+_1$ and $15/2^+_1 \longrightarrow 11/2^+_1$ electric transitions to a great extent. In the first two processes the modifications are caused by the above mentioned rearrengement of the $\nu = 1$ and $\nu = 3$ configurations in the wave functions of the $5/2^+_1$ and $5/2^+_2$ states.

4.2 Influence of the configurations with seniority $\nu = 1$ and $\nu = 3$ and Nqp ≥ 5

We compare here the PBCS approximation with the LSSM. It is evident that for ^{59}Ni, ^{65}Ni and ^{135}I nuclei both calculations lead to identical results. In the case of ^{61}Ni, ^{63}Ni and ^{137}Cs the differences arise from the effect of five-quasi-particle states with $\nu = 1$ and 3 , while in the remaining nuclei, the LSSM also include the correlations induced by configurations with Nqp > 5.

From the energy spectra shown in Figs. 2 and 3 for ^{61}Ni and ^{63}Ni nuclei one sees that, up to an excitation energy of 2 MeV, the PBCS approximation and the LSSM yield quite similar results. The number of states is the same in both calculations and, except for one inversion in ^{63}Ni, the ordering of the levels is also the same. The differences in excitation energies are smaller than 70 keV in ^{61}Ni and smaller than 40 keV in ^{63}Ni.

The calculations of the electromagnetic properties for the above mentioned nuclei, displayed in Figs. 10-13, allow to see that one obtains identical results within PBCS approach and the LSSM for:

1) magnetic dipole moments of the states $3/2^-_1$, $5/2^-_1$ and $7/2^-_1$;
2) electric quadrupole moments of the states $3/2^-_1$ and $5/2^-_1$;
3) B(M1) values for the transitions initiated in the states $1/2^-_1$, $3/2^-_1$, $5/2^-_1$, $7/2^-_1$, $9/2^-_1$, $1/2^-_2$, $3/2^-_2$ and $5/2^-_2$; and
4) B(E2) values for the transitions which involve the states $1/2^-_1$, $3/2^-_1$, $5/2^-_1$, $7/2^-_1$, $3/2^-_2$ and $5/2^-_2$.

Moreover, the corresponding differences for the remaining observables analyzed in the present work, are, for all practical purposes, of minor importance. For example, the magnetic moments differ only up to 0.15 n.m..

The energy spectra of the N = 82 nuclei, represented in Figs. 6-9 up to an excitation energy of 2 MeV, clearly demonstrate that the effects induced by low-seniority configurations with Nqp $\geq$ 5 are relatively small. As a matter of fact, the LSSM and the PBCS calculations generate the same number of states, the ordering of levels is practically the same and the energy differences are $\leq$ 50 keV.

To some extent the above statement is also valid for the electromagnetic properties illustrated in Figs. 14-16. There is no difference worthwhile to be mentioned for the magnetic moments and transitions, as well as, for the electric observables when these involve states with $\bar{\nu} \simeq 1$, i.e., the levels $5/2^{\pm}_1$ and $7/2^{+}_1$. The differences are also small for the quadrupole moments of the remaining low-lying states and the B(E2)-values between states with $\bar{\nu} \simeq 1$ and $\bar{\nu} \simeq 3$. Only when both the initial and the final states are build up dominantely from $\nu = 3$ configurations, the E2 transitions evaluated within the PBCS approximation are, in general, appreciable less collective than those obatined within the LSSM.

4.3 Correlations induced by the blocking effect and the particle-number projection

We still have to analyse and to discuss the correlations induced by the BBCS and PBCS approximations with respect to the usual BCS approach. As reference frame we will always use the LSSM. It is clear that in the case of three valence particles it is not profitable to go to the BCS representation. More precisely, in such a situation, it is easier to perform the shell model calculation than make use of any of the BCS approximations. Therefore we will limit our discussion to nuclei with more than three valence particles. However, and only for the sake of completeness, the results for ^{59}Ni, ^{65}Ni and ^{135}I nuclei are also shown in figures and tables of the present work.

For the energy spectra of ^{61}Ni and ^{63}Ni nuclei up to an excitation energy of 2 MeV there is no difference worthwhile to be mentioned among the BCS, BBCS and PBCS approximations (see Figs. 2 and 3). Above 2 MeV, and when compared with the LSSM, the ordering of the states starts to be different for all three BCS approximations. The best agreement is obtained with the PBCS method and the poorest one within the BCS approach. The largest discrepances in excitation energies up to 3 MeV are of the order of 250 keV.

In Table 3 are listed the wave functions of a few low-lying states in ^{61}Ni and ^{63}Ni obtained with different BCS approaches. One sees that for dominantly $\nu = 1$ states ($1/2^{-}_1$, $3/2^{-}_1$ and $5/2^{-}_1$) the wave functions are not very sensitive neither to the

blocking effect nor to the particle number projection. Contrarely, the wave functions of the remaining states are rather susceptible to both effects. It should be noted that the BBCS wave functions are more resembling to the corresponding PBCS wave functions than the BCS ones. On the other hand, the differences in amplitudes of the wave functions are more pronounced for ^{61}Ni than for ^{63}Ni. For the first nucleus they are of the order of 10%, but may be as large as 25% (compare, for example, the amplitude of the $[(p3/2)^2 4, p1/2]$ configuration in the $7/2_1^-$ state). In the second case the differences are of the order of 4%.

The just mentioned model dependence of the wave functions are reflected in the magnitudes of the electromagnetic observables presented in Figs. 10-13. This dependence is more outstanding for the electric observables than for the magnetic ones. When compared with the LSSM the BCS approximation exhibits significant differences in magnitudes of several moments and transitions which involve the level $7/2_1^-$ in ^{61}Ni nucleus ($\mu(7/2_1^-)$, $Q(7/2_1^-)$, $B(M1;\ 7/2_1^- \rightarrow 5/2_1^-)$ and $B(E2;\ 7/2_1^- \rightarrow 3/2_1^-)$) and the level $3/2_2^-$ in ^{63}Ni nucleus ($Q(3/2_2^-)$, $B(M1;\ 3/2_2^- \rightarrow 3/2_1^-)$ and $B(E2;\ 3/2_2^- \rightarrow 5/2_1^-)$). For both nuclei the PBCS results are more close to the LSSM calculations than those which one gets within the BBCS approach.

From the energy spectra of N = 82 nuclei, displayed in Figs. 6-9 it can be seen that the simple-minded BCS calculations, when compared with the results of the LSSM, yield significant differences (up to ≈ 300 keV) for the excitation

energies of several states, as well as, they give way to quite different level orderings. The last effect is particularly accentuated in the energy region where the level density is rather high. Although both the BBCS and the PBCS approaches provide satisfactory results for the energy spectra, the agreement with the LSSM calculations is somewhat better in the second case.

In Table 6 are confronted the wave functions, calculated with different BCS approximations, for N = 82 isotones with more than five valence particles. For dominantely 1QP states, i.e., $5/2_1^+$ and $7/2_1^+$ levels, all three calculations yield analogous wave function amplitudes. For the remaining states only the BBCS and PBCS amplitudes are close to each other. The most noticeable differences between the BBCS (or PBCS) wave functions occur for the $[(7/2)^2 J_{12}, 5/2]$ configurations in ^{139}La and for the $[(5/2)^2 J_{12}, 7/2]$ configurations in ^{141}Pr.

The results for the electromagnetic properties calculated with the just mentioned wave functions are compared with the LSSM results in Figs. 14-16. It is seen that all four models furnish similar results for the magnetic observables. The most notable discrepancy is found in tne BCS value for the $13/2_1^+ \rightarrow 11/2_1^+$ M1 transition in ^{139}La. Among all BCS results for the electric observables only that for $Q(5/2_1^+)$, $Q(7/2_1^+)$ and $B(E2;\ 5/2_1^+ \rightarrow 7/2_1^+)$ come together to the LSSM results. At variance, the quadrupole obtained within the remaining two BCS approximations are not substantially different from those evaluated within the LSSM. With respect to the B(E2) values it should be noted that the

best overall agreement is achieved with the number-projection method. It is also important to be mentioned that when a B(E2) value strongly fluctuate in going from one nucleus to another, as happens in the case of the $5/2_2^+ \rightarrow 7/2_1^+$, $3/2_1^+ \rightarrow 7/2_1^+$ and $11/2_1^+ \rightarrow 7/2_1^+$ transitions, it turns out that the ordinary BCS calculations lead to more satisfactory results than the BBCS ones.

We have mentioned, in the former part of this section that in most of the cases the electric observables were more sensible to the blocking effect (and to the number projection procedure) than the magnetic ones. In order to clarify this point we will present below a qualitative discussion of the matrix elements of the one body operator T_λ. We assume that both the initial and final wavefunctions are dominantely 1QP or 3QP states (see Tables 3 and 6). Therefore the following matrix elements will be appear: i) $\langle\psi(1QP)\| T_\lambda \|\psi'(1QP)\rangle$, ii) $\langle\psi(1QP)\| T_\lambda \|\psi(3QP)\rangle$ and iii) $\langle\psi(3QP)\| T_\lambda \|\psi(3QP)\rangle$. The matrix element of the type i) and iii) are proportional to the scattering pairing factor $F_s(\lambda) \equiv (u_a u'_b - (-)^\lambda v_a v'_b)$ and those of the type ii) to the pair creation pairing factor $F_p(X) \equiv (u'_a v'_B - (-)^\lambda v'_a u'_b)$. One way distinguish two limiting situation:

1) the valence shell is approximately half-filled in which case the electric pairing factors are $F_s(\lambda=2)\approx 0$ and $F_p(X=2)\approx 1$;

2) only a few particles or holes are in the valence shell and therefore $F_s(\lambda=2)\approx 1$ and $F_p(\lambda=2)\approx 0$. In both limiting situation the magnetic pairing factors are $F_s(\lambda=1)\approx 1$ and $F_p(\lambda=1)\approx 0$. On the other hand, the results for the electromagnetic properties shown in Figs.

10-13 and Figs. 14-16, correspond mostly to the case 1) and thus the blocking effect is particularly relevant for the electric observables of types i) and iii) and for the magnetic observables of type iii).

It is clear that the main differences between the BCS and BBCS results come from the differences in the gap parameter. Due to the blocking effect this quantity diminishes and becomes configuration dependent. Moreover, as shown in ref.[17], the pairing reduction depends sensitively on the single-particle level distribution near the Fermi surface and is particularly pronounced when the blocked level is located close to the Fermi surface. Thus, from the results shown in Fig. 17, one can easily conviced oneself that the blocking effect is very important for the following wavefunction amplitudes (and the corresponding electromagnetic observables):

i) configurations which contain two particles in the single particle state $p_{3/2}$ and participate in building up the wavefunctions of ^{61}Ni.

ii) components which involve the orbital $g_{7/2}$ in ^{137}Cs and ^{139}La and the orbital $d_{5/2}$ in ^{141}Pr and ^{143}Pm; the effect is particularly relevant for the configurations $|(7/2)^2 J_{12};5/2\rangle$ in ^{139}La and the configurations $|(5/2)^2 J_{12},7/2\rangle$ in ^{141}Pr.

However, contrarely to what one would expect the structure of ^{137}Cs and ^{143}Pm nuclei seems to be less affected by the blocking effect than that of ^{139}La and ^{141}Pr nuclei (see Fig. 17). This fact indicates that a discussion of the blocking effect

based only on the analysis of a few diagonal matrix elements of H and/or on the most important contributions to T_λ might be a oversimplification and, therefore, far of being totally conclusive. In particular, the calculation of the structure of N = 82 isotones involve a large configuration space with many nondiagonal matrix elements of H and many contributions to the to T_λ which are appreciable different when evaluated within the BCS of BBCS approximations.

5. Conclusions

In this paper a detailed study of shell-model correlations, induced into the BCS approximation by the number projection method and by the blocking effect, has been carried out. Particularly, the low-seniority shell model was used as the frame of reference to investigate the mixing of one and three quasi-particle states in Ni isotopes and in N = 82 isotones. In addition, effects of seniority-five configurations on low-lying states has also been studied through the comparison of low-seniority shell-model results with those which arise from the full shell-model calculations.

The following conclusions, what we believe are of general interest, can be drown from the discussion performed in the preceding section:

1) A BCS approximation which includes the number projection or the blocking effect yields results which are in many respect very close to ones obtained within the low-seniority shell-model.
2) The five-quasiparticle configurations with seniority one and three do not play an important role in the structure of low-lying states.
3) The effect of seniority-five configurations may be quite significant even on the electromagnetic processes among the lowest states and can hardly be taken into account through a overall renormalization of the residual interaction or/and of the effective charges.

We have not presented here the comparison between the

experimental data and the calculations. However, it should be noted that, with the parametrization listed in section 3, the complete shell model yields a fairly well overall agreement with the experiments.

Last but not least we would like to point out that several calculations, which include at the same time the number projection and the blocking effect, have also been performed. Such a procedure, in spite of being significantly more time consuming than the BBCS and PBCS methods separately, does not exhibit any advantage worthwhile to be quoted. Thus it does not seem to be profitable to consider at the same time the blocking effect and the number projection.

REFERENCES

1) T.T.S. Kuo, E.U. Baranger and M. Baranger, Nucl. Phys. 79 (1966) 513.

2) K. Dietrich, H.J. Mang and J.H. Pradal, Phys. Rev. 135 (1964) 322.

3) P.L. Ottaviani and M. Savoia, Phys. Rev. 187 (1969) 1306; Nuovo Cim. 67A (1970) 630; Phys. Rev. 178 (1969) 1594.

4) K. Allaart and E. Boeker, Nucl. Phys. A168 (1971) 630; Nucl. Phys. A198 (1972) 33.

5) K. Allaart and W.F. Van Gunsteren, Nucl. Phys. A234 (1974) 53.

6) I.N.L. Akkermans, K. Allaart and Z. Boeker, Nucl. Phys. A282 (1977) 291.

7) S.G. Nilsson, Nucl. Phys. 55 (1964) 97.

8) H. Dias and F. Krmpotić, Phys. Lett. 112B (1982) 103.

9) L. Losano, H. Dias, F. Krmpotić and B.H. Wildenthal, to be published.

10) J.B. French, E.C. Halbert, J.B. Mcgrory and S.S.M. Wong, Advances in Nuclear Physics, vol. 3 (1969) 193.

11) M.H. Macfarlane, Lectures in Theoretical Physics, University of Colorado Press, Boulder (1966) 583.

12) H. Dias, Ph.D. Thesis, University of São Paulo (1980).

13) A. Plastino, R. Arvieu and S.A. Moskowski, Phys. Rev. 145 (1966) 837.

14) N. Freed and N. Miles, Nucl. Phys. A167 (1970) 230.

15) L.S. Kisslinger and R.A. Sorensen, Rev. Mod. Phys. 35 (1963) 853.

16) J.E. Koops and P.W.M. Glaudemans, Z. Phys. A280 (1977) 181.

17) J.Y. Zeng, T.S. Cheng, L. Cheng and C.S. Wu, Nucl. Phys. A411 (1983) 49.

TABLE CAPTIONS

TABLE 1 - Dimensions for some negative parity states of Ni isotopes using the approaches CSM and LSSM. For differents BCS calculations the size configurations for all isotopes are equal to the numbers given in the second column. See text for details.

TABLE 2 - Dimensions for some positive parity states of N = 82 isotones. See table 1 caption.

TABLE 3 - Calculated wave functions of some low-lying states in ^{61,63}Ni nuclei using differents BCS approaches. The basis states are $|(j_a j_b)J_{ab}, j_c, J\rangle$. Only amplitudes larger than 4% are listed.

TABLE 4 - For some selected states in ^{61}Ni are given the seniority (ν) decomposition in percent (%) and the average seniority using the approaches CSM and LSSM.

TABLE 5 - The same information described in table 4 caption for ^{63}Ni.

TABLE 6 - Calculated wave functions of same low-lying states in ^{137}Cs, ^{139}La, ^{141}Pr and ^{143}Pm. See table 3 caption for details.

TABLE 7 - The same information described in table 4 caption for ^{137}Cs.

FIGURE CAPTIONS

FIGURE 1 - The calculated energy levels for the negative parity states in ^{59}Ni using differents approaches (see text for details). The spins are in 2J form. In this case the results with CSM, LSSM and PBCS are identical.

FIGURE 2 - Energy levels of ^{61}Ni. For further explanation see Fig. 1 caption.

FIGURE 3 - Energy levels of ^{63}Ni. For further explanation see Fig. 1 caption.

FIGURE 4 - Energy levels of ^{65}Ni. For further explanation see Fig. 1 caption.

FIGURE 5 - The calculated energy levels for the positive parity states in ^{135}I using differents approaches (see text for details). The spins are in 2J form. In this case the results with CSM, LSSM and PBCS are identical.

FIGURE 6 - Energy levels of ^{137}Cs. For further explanation see Fig. 5 caption.

FIGURE 7 - Energy levels of ^{139}La. For further explanation see Fig. 5 caption.

FIGURE 8 - Energy levels of ^{141}Pr. For further explanation see Fig. 5 caption.

FIGURE 9 - Energy levels of ^{143}Pm. For further explanation see Fig. 5 caption.

FIGURE 10 - The calculated magnetic dipole moments in (n.m.) units for some lowest levels as a function of the mass number in Ni isotopes ($59 \leqslant A \leqslant 65$). The results within the CSM, LSSM, BCS, BBCS and PBCS approximations are labeled with letters A,B,C,D and E, respectively.

FIGURE 11 - The calculated electric quadrupole moments in e.fm^2 units for some levels as a function of the mass number in Ni isotopes ($59 \leqslant A \leqslant 65$). For further explanation see Fig. 10 caption.

FIGURE 12 - The calculated magnetic M1 transition rates in 10^{-2} Wu units for some transitions as a function of the mass number in Ni isotopes ($59 \leqslant A \leqslant 65$). For further explanation see Fig. 10 caption.

FIGURE 13 - The calculated electric E2 transition rates in Wu units for some transitions as a function of the mass number in Ni isotopes ($59 \leqslant A \leqslant 65$). For further explanation see Fig. 10 caption.

FIGURE 14 - The calculated magnetic dipole moments in n.m. units for some lowest levels as a function of the mass number in N = 82 isotones ($135 \leqslant A \leqslant 143$). The calculated magnetic M1 transition rates in 10^{-2} Wu units for two transitions are also presented. The results within the LSSM, BCS, BBCS and PBCS approximations are labeled with letters A,B,C and D, respectively. The results calculated within the framework of CSM are represented by open circles. The remaining M1 transitions will not discuss since all they are very weak (10^{-3} Wu) as a consequence of the l-forbiddeness.

FIGURE 15 - The calculated electric quadrupole moments in e.fm^2 units for some levels as a function of the mass number in N = 82 isotopes ($135 \leqslant A \leqslant 143$). For further explanation see Fig. 14 caption.

FIGURA 16 - The calculated electric E2 transition rates in Wu units for some transitions as a function of the mass number in N = 82 isotone ($135 \leqslant A \leqslant 143$). For further explanation see Fig. 14 caption.

FIGURA 17 - Single particle energies (continuous line) and Fermi energies (dashed line) $\lambda(n_0)$ where n_0 is the number of nucleons. In (a) for Ni isotopes and (b) for N = 82 isotones.

TABLE 1

	$^{59,65}Ni$	$^{61,63}Ni$	
SPIN	CSM - BCS	CSM	LSSM
1/2	5	15	10
3/2	10	24	18
5/2	10	29	20
7/2	6	23	14
9/2	5	17	11
11/2	1	8	3

TABLE 2

	^{135}I	^{137}Cs		^{139}La		^{141}Pr and ^{143}Pm	
SPIN	CSM-BCS	CSM	LSSM	CSM	LSSM	CSM	LSSM
1/2	12	107	39	415	73	790	96
3/2	25	198	80	764	149	1484	198
5/2	28	253	93	1005	174	1965	231
7/2	27	271	91	1121	173	2215	231
9/2	23	252	82	1091	159	2214	215
11/2	16	211	59	974	117	2017	160
13/2	8	153	30	783	62	1669	86
15/2	5	105	20	577	41	1284	57

TABLE 3

					^{61}Ni			^{63}Ni		
J_i	j_a	j_b	J_{ab}	j_c	BCS	BBCS	PBCS	BCS	BBCS	PBCS
$3/2_1$				3/2	.960	.961	.968	.953	.961	.956
$5/2_1$				5/2	.981	.979	.984	.987	.986	.992
$1/2_1$				1/2	.890	.895	.834	.941	.940	.948
	3/2	3/2	0	1/2						
	3/2	3/2	2	5/2	.203	.196	.208			
	3/2	1/2	2	5/2	-.276	-.265	-.295			
	5/2	5/2	2	3/2	.226	.224	.250			
$3/2_2$				3/2	.198	.224	.206			.214
	3/2	3/2	0	3/2	.194	.257	.268			
	5/2	5/2	2	1/2	.528	.416	.411	.634	.633	.620
	3/2	3/2	2	5/2	-.317	-.340	-.340	-.240	-.217	-.218
	3/2	1/2	2	5/2	.483	.559	.579	.397	.396	.384
	5/2	5/2	2	5/2	.517	.443	.439	.563	.586	.594
$1/2_2$				1/2	-.455	-.446	-.463	.338	.341	.316
	3/2	3/2	0	1/2	-.306	-.306	-.435	.344	.353	.432
	5/2	5/2	0	1/2	.254	.276	-	.231	.242	-
	5/2	5/2	2	3/2	.444	.463	.451	-.473	-.465	-.473
	3/2	3/2	2	5/2	.407	.397	.368	-.377	-.345	-.345
	3/2	1/2	2	5/2	-.522	-.510	-.508	.590	.604	.609
$5/2_2$										
	1/2	1/2	0	5/2				.353	.328	.462
	3/2	3/2	0	5/2	.268	.220	.361			
	5/2	5/2	0	5/2	-.305	-.201	-	-.343	-.338	-
	3/2	5/2	2	5/2	-.557	-.478	-.472			
	5/2	5/2	2	3/2	.419	.556	.547			
	3/2	3/2	2	1/2	.398	.489	.466			
	5/2	5/2	2	1/2	-.221			-.609	-.584	-.615
	3/2	1/2	1	5/2	.231	.307	.288			
	3/2	1/2	2	5/2				-.512	-.572	-.540
	5/2	5/2	4	3/2				.240	.227	.240
	3/2	3/2	2	5/2				.216		
$7/2_1$										
	5/2	5/2	2	3/2	.418	.630	.624	.328	.362	.346
	3/2	1/2	2	5/2	.453	.525	.520	.418	.444	.437
	3/2	3/2	4	1/2	.629	.399	.385			
	5/2	5/2	4	3/2	.312	.222	.272	.266	.250	.261
	3/2	3/2	2	5/2	-.341			-.255	-.200	-.217
	3/2	1/2	1	5/2		-.313	-.306			
	5/2	5/2	4	1/2				.761	.750	.755

TABLE 4

	$\nu = 1$ (%)		$\nu = 3$ (%)		$\nu = 5$ (%)	$\bar{\nu}$	
SPIN	CSM	LSSM	CSM	LSSM	CSM	CSM	LSSM
$5/2_1$	95.58	97.01	3.66	2.99	0.76	1.10	1.06
$3/2_1$	93.80	94.01	6.15	5.99	0.05	1.12	1.12
$1/2_1$	79.89	80.47	19.84	19.53	0.27	1.41	1.39
$3/2_2$	10.90	11.86	88.67	88.14	0.43	2.78	2.76
$1/2_2$	42.57	40.80	56.53	59.20	0.90	2.17	2.18
$5/2_2$	15.81	14.62	72.96	85.38	11.23	2.91	2.71
$7/2_1$	0.	0.	94.90	100.	5.10	3.10	3.
$3/2_3$	18.84	18.33	60.92	81.67	20.24	3.03	2.63
$5/2_3$	23.68	15.96	52.65	84.04	23.67	2.99	2.68
$7/2_2$	0.	0.	91.86	100.	8.14	3.16	3.
$5/2_4$	11.59	-	80.73	-	7.68	2.94	-
$9/2_1$	0.	0.	98.69	100.	1.31	3.03	3.
$9/2_2$	0.	0.	84.03	100.	15.97	3.32	3.
$7/2_3$	0.	-	68.21	-	31.79	3.64	-
$11/2_1$	0.	0.	97.68	100.	2.32	3.05	3.
$3/2_4$	6.34	-	46.51	-	47.15	3.83	-
$1/2_3$	11.60	-	57.40	-	31.00	3.40	-
$5/2_5$	8.84	-	53.63	-	37.53	3.46	-

TABLE 5

	ν = 1 (%)		ν = 3 (%)		ν = 5 (%)	$\bar{\nu}$	
SPIN	CSM	LSSM	CSM	LSSM	CSM	CSM	LSSM
$1/2_1$	90.46	90.65	9.49	9.35	0.05	1.19	1.19
$5/2_1$	98.09	98.43	1.77	1.57	0.14	1.04	1.03
$3/2_1$	89.30	91.20	10.68	8.80	0.02	1.21	1.18
$3/2_2$	8.04	6.88	88.07	93.12	3.89	2.92	2.86
$1/2_2$	29.14	28.76	70.44	71.24	0.42	2.43	2.43
$7/2_1$	0.	0.	94.45	100.	5.55	3.11	3.
$5/2_2$	24.14	23.41	66.46	76.59	9.40	2.71	2.53
$3/2_3$	13.72	17.50	71.84	82.50	14.44	3.01	2.65
$5/2_3$	6.80	8.11	80.51	91.89	12.69	3.12	2.84
$9/2_1$	0.	0.	94.43	100.	5.57	3.11	3.
$7/2_2$	0.	0.	87.15	100.	12.85	3.26	3.
$5/2_4$	21.53	-	45.94	-	32.53	3.22	-
$7/2_3$	0.	-	72.23	100.	27.77	3.56	-
$3/2_4$	9.89	-	66.54	-	23.57	3.28	-
$9/2_2$	0.	0.	86.14	100.	13.86	3.28	3.
$5/2_5$	3.99	-	54.49	-	41.52	3.75	-

TABLE 6

					^{137}Cs			^{139}La			^{141}Pr			^{143}Pm		
J_i	j_a	j_b	J_{ab}	J_c	BCS	BBCS	PBCS	BCS	BBCS	PBCS	BCS	BBCS	PBCS	BCS	BBCS	PBCS
$7/2_1$				7/2	.986	.983	.991	.980	.978	.984	.979	.981	.980	.980	.981	.979
$5/2_1$				5/2	.984	.986	.982	.985	.987	.987	.985	.983	.988	.987	.986	.984
$3/2_1$				3/2				.210	.238	.265	.535	.332	.442			
	7/2	7/2	2	5/2				.519	.713	.677		.278	.209			
	5/2	5/2	2	7/2				.210	.422	.407	.677	.744	.759			
	7/2	7/2	4	7/2	.962	.978	.963	-.463								
	7/2	7/2	4	5/2				.212	.349	.404	.271		.205			
	5/2	5/2	4	7/2				.264								
	5/2	5/2	4	5/2				-.471				.353		.947	.953	.956
$1/2_1$				1/2				.288		.215	.480	.357	.407	.915	.899	.851
	7/2	7/2	2	5/2	-.891	-.917	-.914	-.822	-.908	-.893	-.587	-.480	-.444	-.200		-.212
	5/2	5/2	4	7/2	.307	.260	.261	.407	.299	.308	.586	.765	.749	.293	.366	.424
	7/2	5/2	1	3/2				.200			.211					
$9/2_1$																
	7/2	7/2	2	5/2				.918	.982	.954						
	5/2	5/2	2	7/2							.945	.969	.955			
	7/2	7/2	4	7/2	.955	.971	.957									
	7/2	7/2	4	5/2	.210	.179	.207			.230						
	5/2	5/2	4	7/2										-.230	-.210	-.463
	5/2	5/2	4	5/2				-.278						.951	.953	.969
$11/2_1$																
	5/2	5/2	2	7/2							.933	.987	.952	.920	.902	.907
	7/2	7/2	4	7/2	.940	.960	.942									
	7/2	7/2	4	5/2				.926	.983	.983						
	5/2	5/2	4	7/2							.269		.255	.338	.382	.362
	7/2	7/2	6	5/2	.231	.195	.230									
$7/2_2$																
	7/2	7/2	0	7/2				-.467		-.321						
	5/2	5/2	0	5/2				.528								
	7/2	7/2	2	5/2	.959	.968	.969	.643	.944	.927						
	5/2	5/2	2	7/2							.813	.806	.840	.855	.886	.878
	7/2	7/2	4	5/2							-.237					
	5/2	5/2	4	7/2							-.391	-.505	-.437	-.396	-.360	-.357
$5/2_2$																
	7/2	7/2	0	5/2				-.290			.596	.419	.796	-.604	-.573	-.360
	5/2	5/2	0	5/2				.468	.267		-.615	-.464		.470	.381	
	7/2	7/2	2	5/2				-.742	-.730	-.821	.240	.243	.203	-.240		-.208
	5/2	5/2	2	7/2				.232	.349	.277	-.314	-.685	-.467	.475	.626	.816
	7/2	7/2	4	7/2	.953	.971	.950		.279							
	7/2	7/2	4	5/2					.361	.397						

TABLE 7

	ν = 1 (%)		ν = 3 (%)		ν = 5 (%)	$\bar{\nu}$	
SPIN	CSM	LSSM	CSM	LSSM	CSM	CSM	LSSM
$7/2_1$	97.75	98.22	2.07	1.78	0.18	1.05	1.04
$5/2_1$	90.48	96.02	9.40	3.98	0.12	1.20	1.08
$5/2_2$	7.17	2.28	89.17	97.72	3.66	2.96	2.95
$3/2_1$	0.00	0.00	95.28	100.00	4.72	3.08	3.00
$11/2_1$	-	-	94.00	100.00	6.00	3.11	3.00
$9/2_1$	-	-	93.98	100.00	6.02	3.11	3.00
$15/2_1$	-	-	96.03	100.00	3.97	3.08	3.00
$1/2_1$	3.07	3.59	93.04	96.41	3.89	3.02	2.93
$9/2_2$	-	-	96.45	100.00	3.55	3.10	3.00
$7/2_2$	0.60	1.20	94.74	98.80	4.66	3.06	2.98
$3/2_2$	3.07	3.86	93.63	96.14	3.30	3.03	2.92
$5/2_2$	1.74	1.50	95.10	98.50	3.16	3.06	2.97
$13/2_1$	-	-	94.99	100.00	5.01	3.10	3.00
$11/2_2$	-	-	97.75	100.00	2.25	3.06	3.00
$15/2_2$	-	-	90.47	100.00	9.53	3.19	3.00
$9/2_3$	-	-	85.14	100.00	14.86	3.33	3.00
$3/2_3$	1.59	1.73	94.19	98.27	5.81	3.11	2.96
$7/2_3$	1.15	4.71	97.70	95.29	8.67	3.19	2.91
$11/2_3$	-	-	80.87	100.00	19.13	3.41	3.00
$5/2_4$	3.17	4.47	86.88	95.53	9.95	3.17	2.91
$7/2_4$	48.20	41.47	48.79	58.53	3.01	2.13	2.16
$13/2_2$	-	-	54.24	100.00	45.76	3.91	3.00
$9/2_4$	-	-	93.68	100.00	6.32	3.16	3.00
$13/2_3$	-	-	33.51	100.00	66.49	4.32	3.00

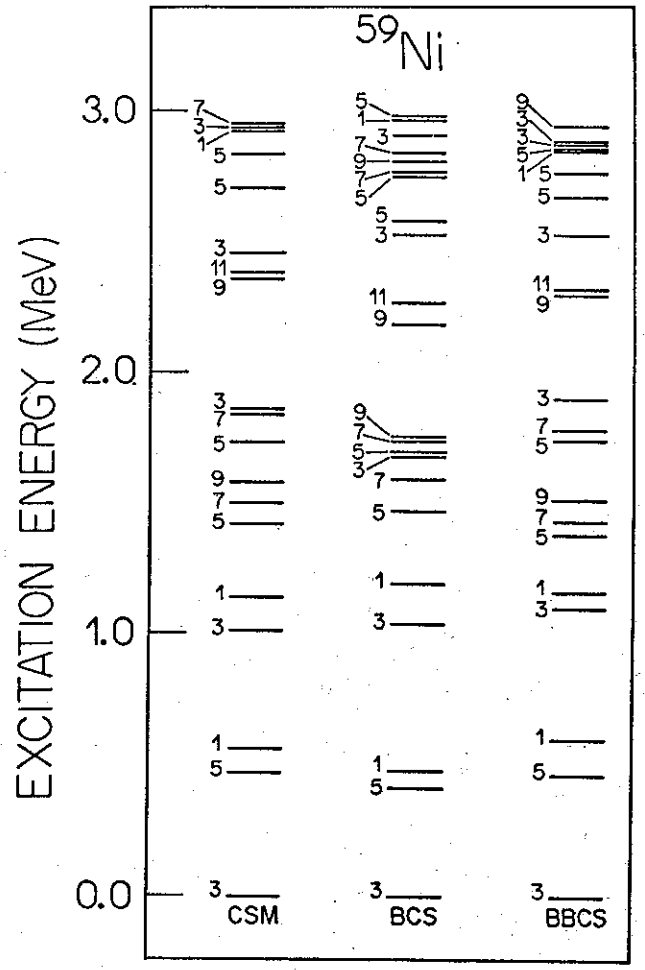

Fig. 1

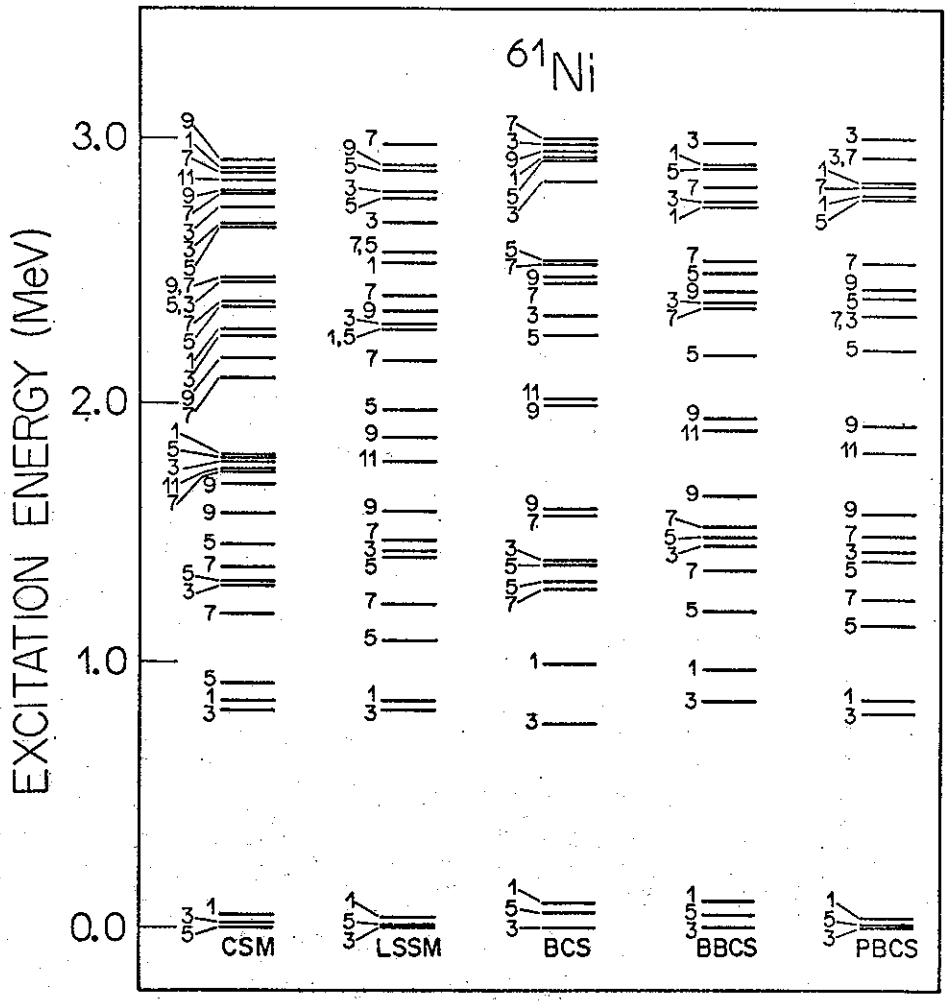
^{61}Ni
EXCITATION ENERGY (MeV)
3.0
2.0
1.0
0.0
CSM
LSSM
BCS
BBCS
PBCS

Fig. 2

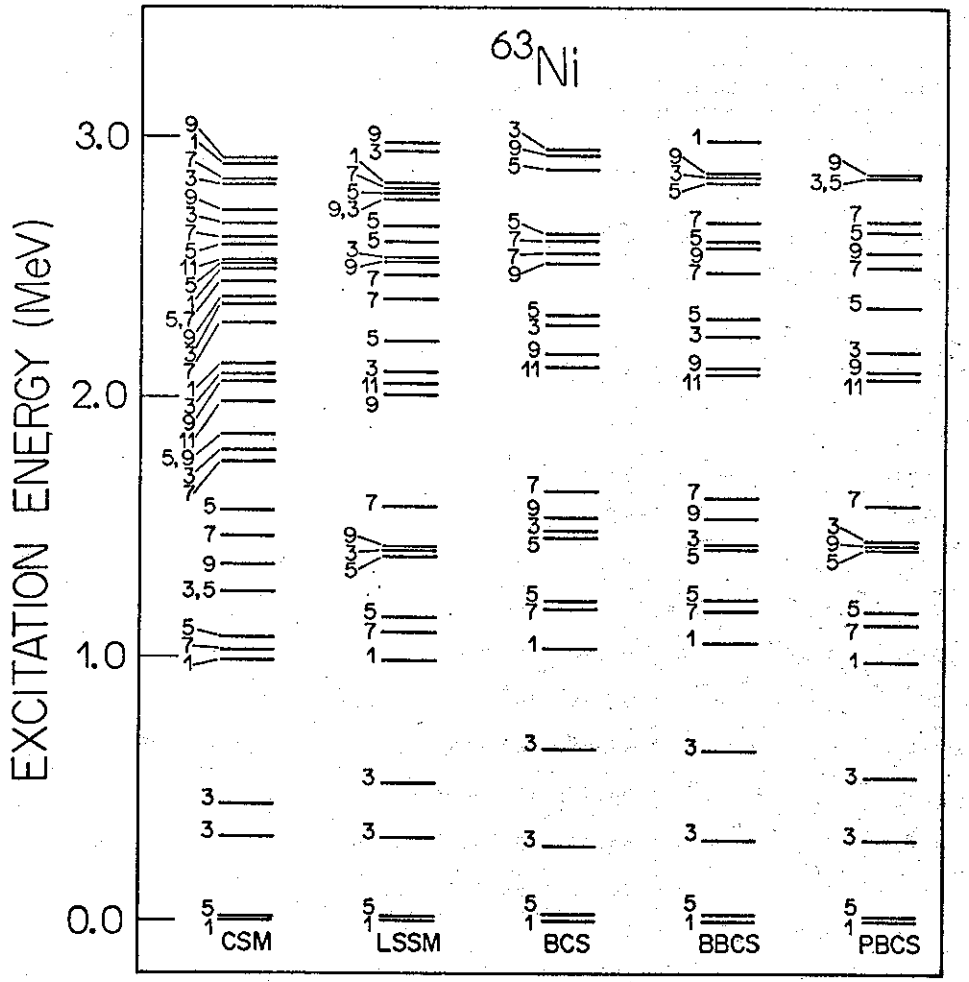
^{63}Ni
EXCITATION ENERGY (MeV)
3.0
2.0
1.0
0.0
CSM
LSSM
BCS
BBCS
PBCS

Fig. 3

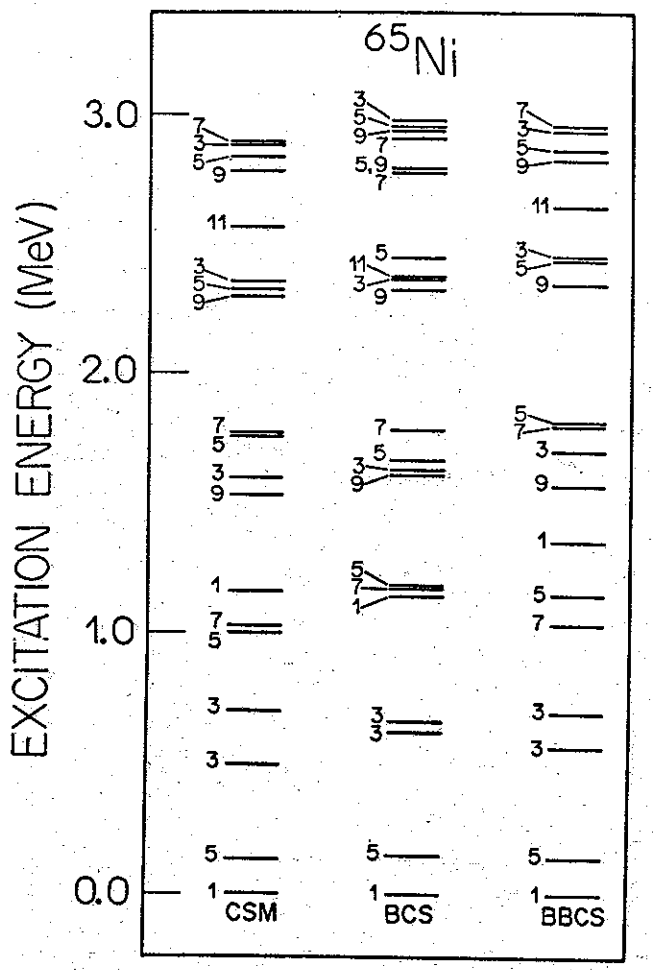
^{65}Ni
EXCITATION ENERGY (MeV)
3.0
2.0
1.0
0.0
CSM
BCS
BBCS

Fig. 4

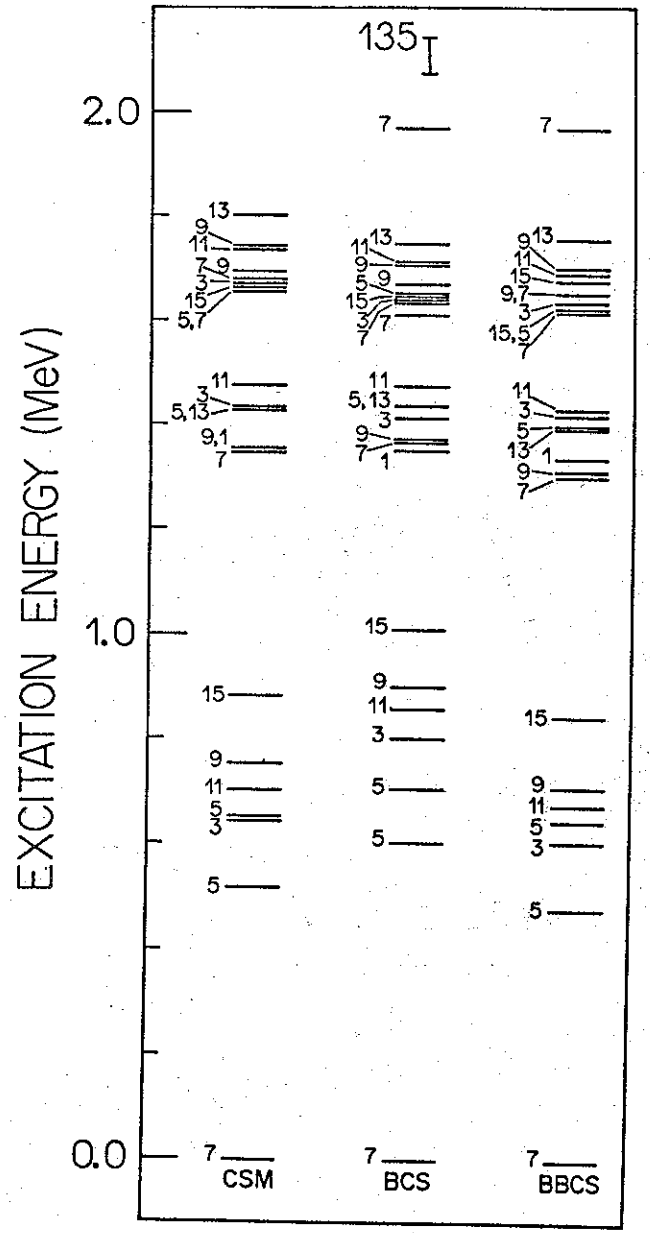
^{135}I
EXCITATION ENERGY (MeV)
2.0
1.0
0.0
CSM
BCS
BBCS

Fig. 5

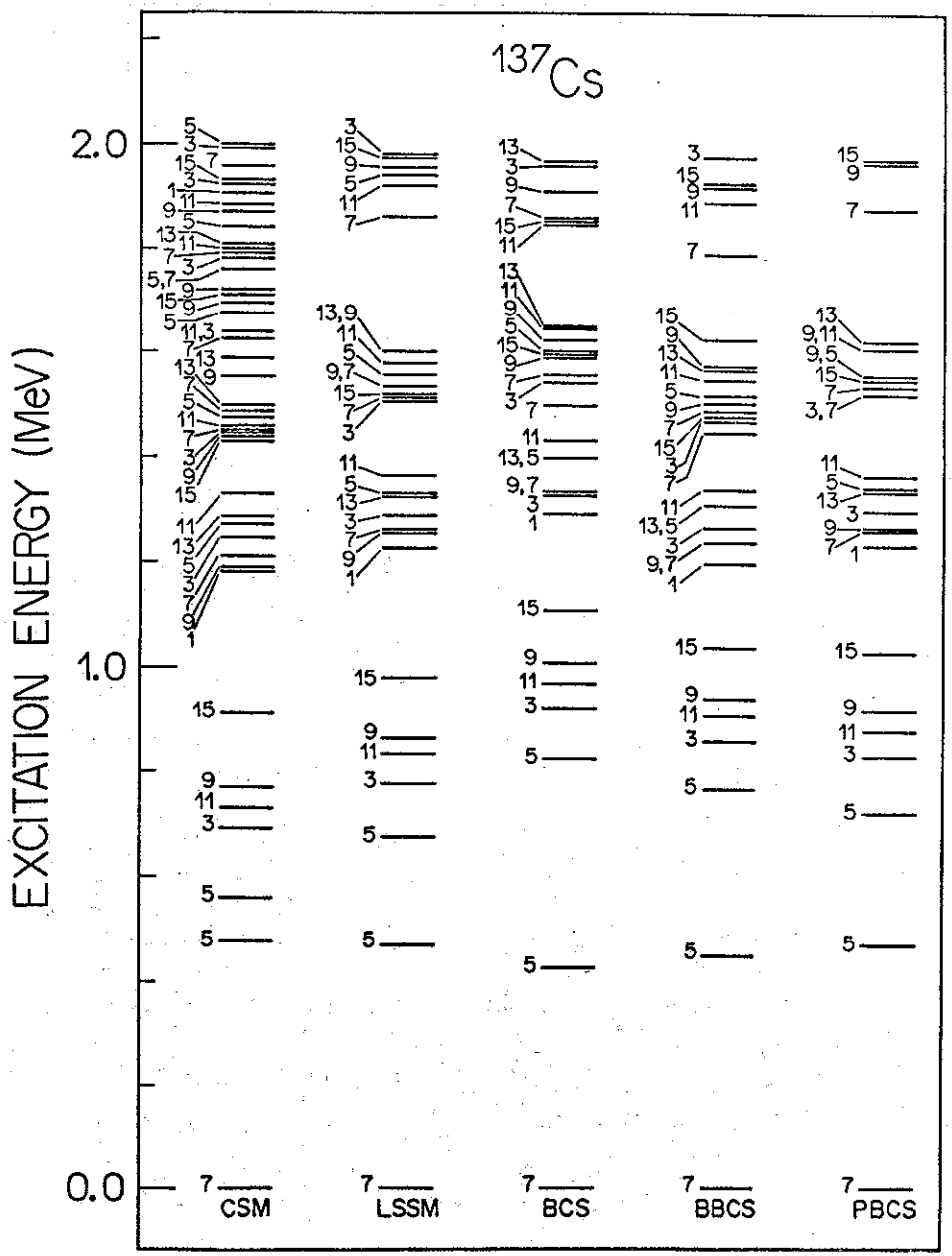
^{137}Cs
EXCITATION ENERGY (MeV)
2.0
1.0
0.0
CSM
LSSM
BCS
BBCS
PBCS

Fig. 6

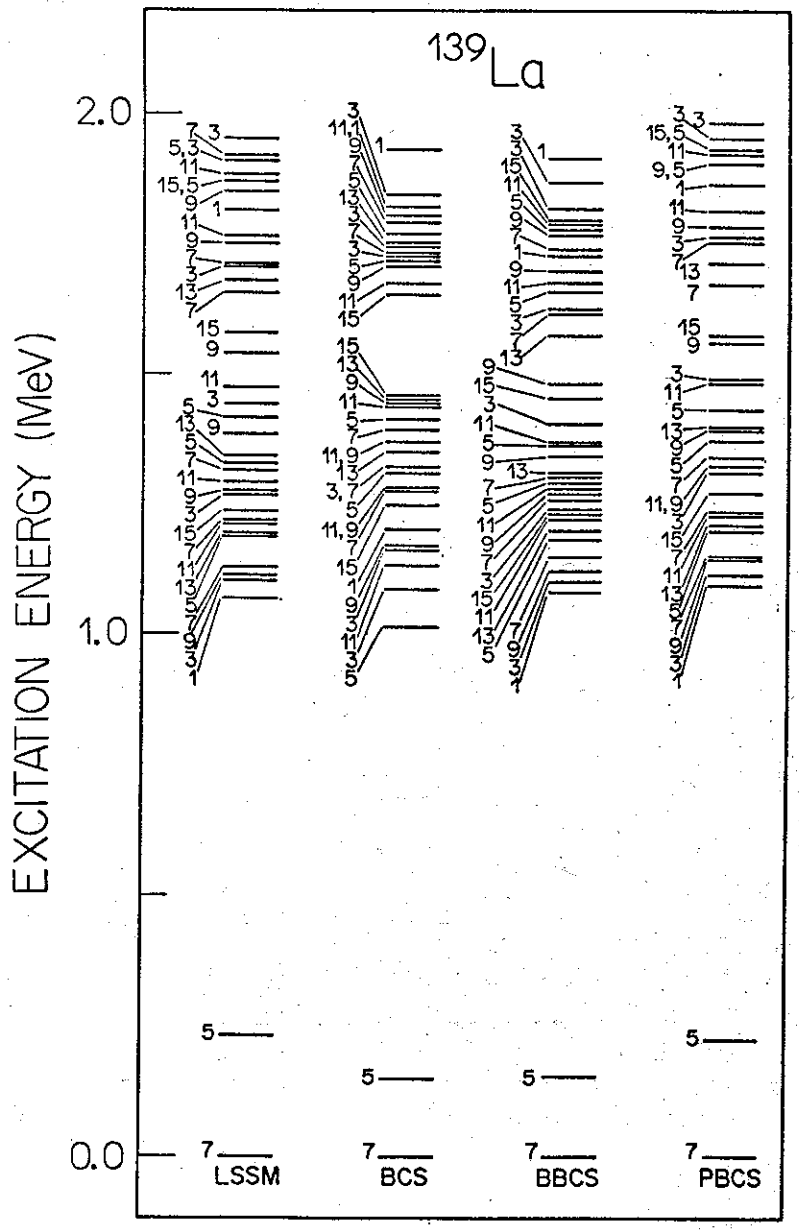
^{139}La
EXCITATION ENERGY (MeV)
2.0
1.0
0.0
LSSM
BCS
BBCS
PBCS

Fig. 7

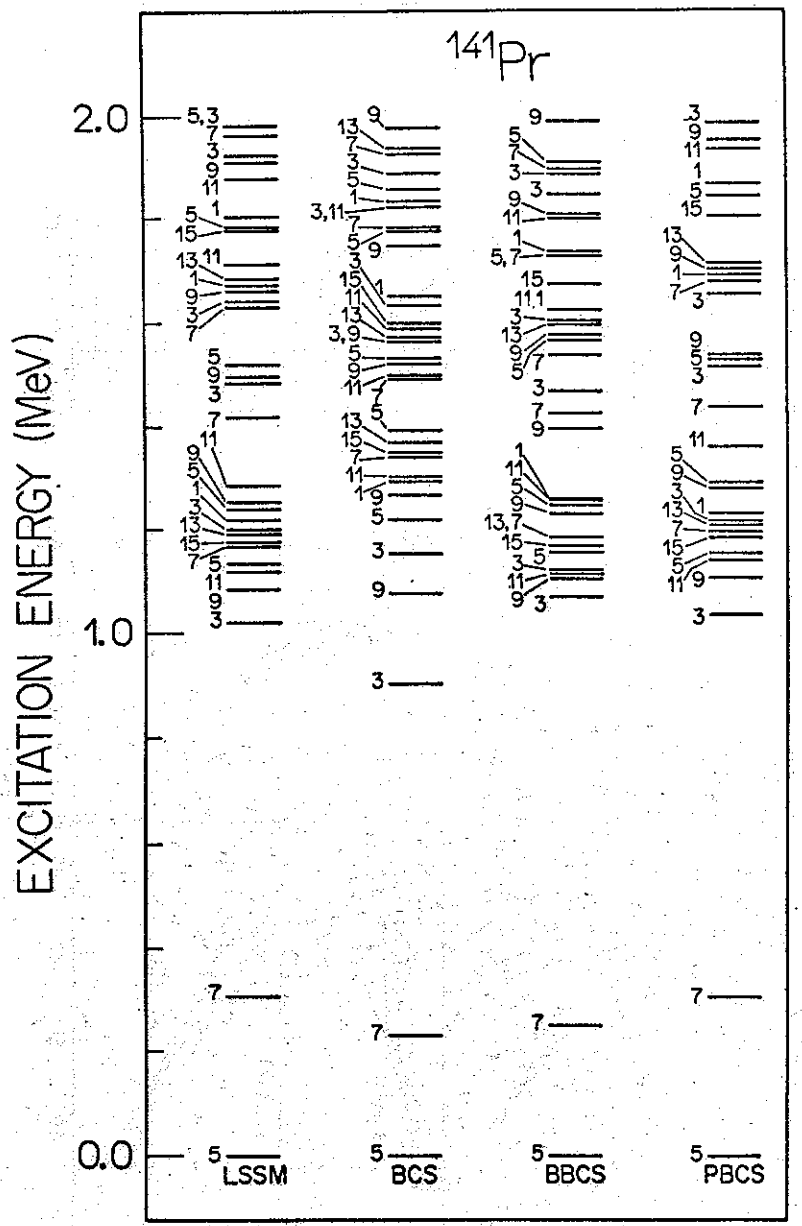
141Pr
EXCITATION ENERGY (MeV)
2.0
1.0
0.0
LSSM
BCS
BBCS
PBCS

Fig. 8

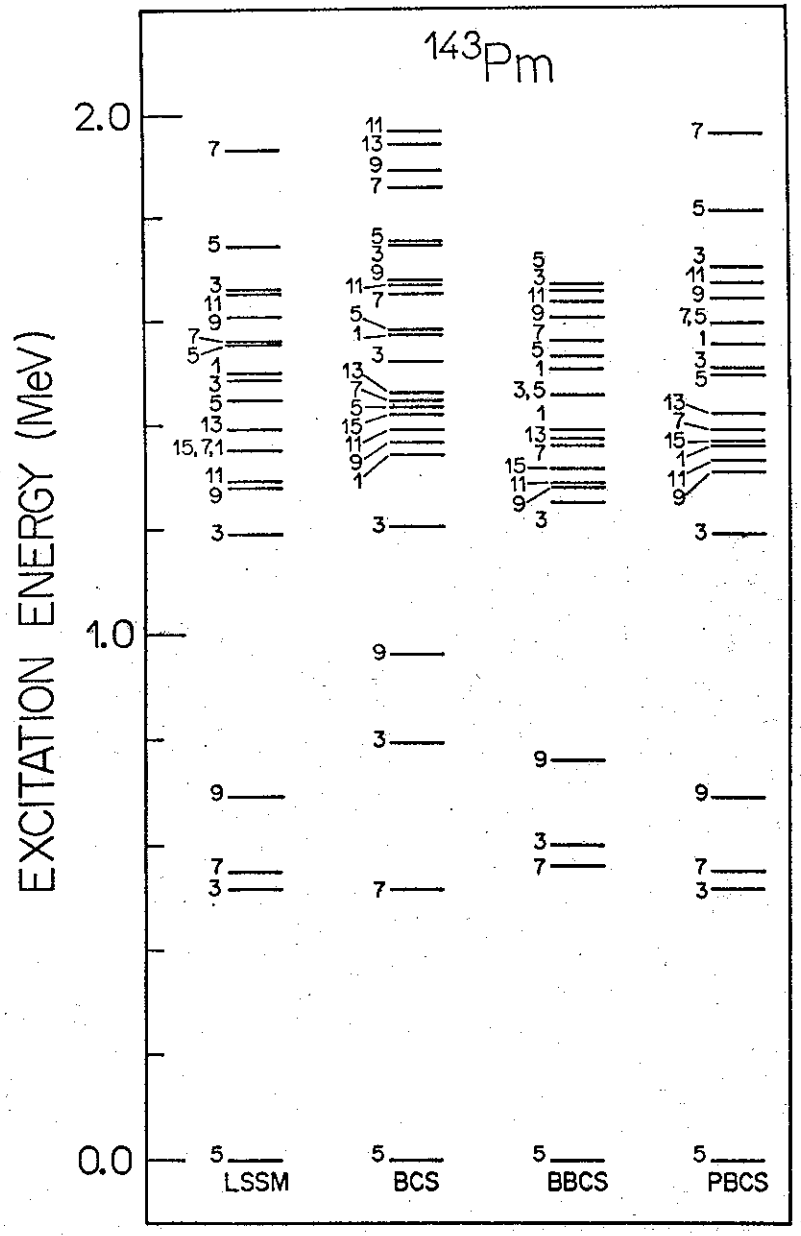
143Pm
EXCITATION ENERGY (MeV)
2.0
1.0
0.0
LSSM
BCS
BBCS
PBCS

Fig. 9

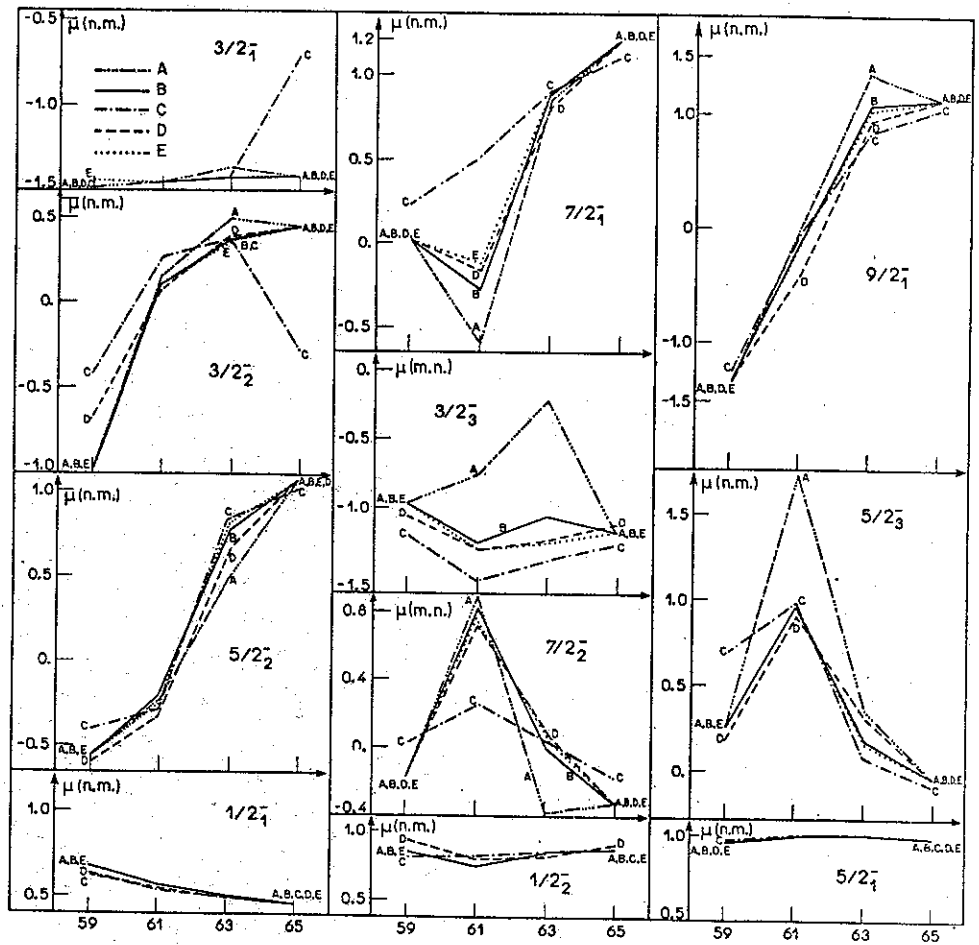
μ (n.m.)
3/2₁⁻
7/2₁⁻
9/2₁⁻
3/2₂⁻
3/2₃⁻
5/2₂⁻
7/2₂⁻
5/2₃⁻
1/2₁⁻
1/2₂⁻
5/2₁⁻
A
B
C
D
E

Fig. 10

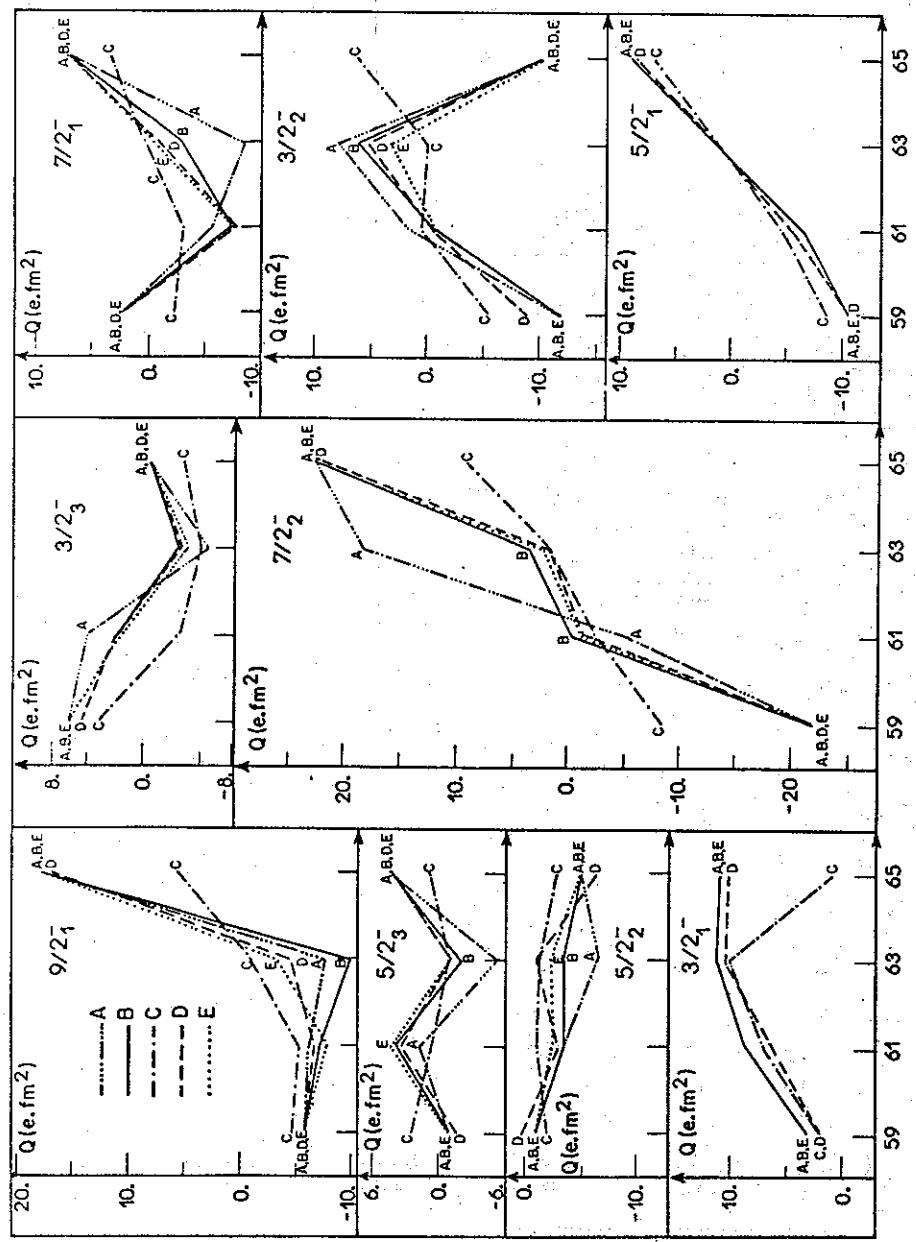
Q (e.fm²)
7/2₁⁻
3/2₂⁻
5/2₁⁻
3/2₃⁻
7/2₂⁻
9/2₁⁻
5/2₃⁻
5/2₂⁻
3/2₁⁻
A
B
C
D
E

Fig. 11

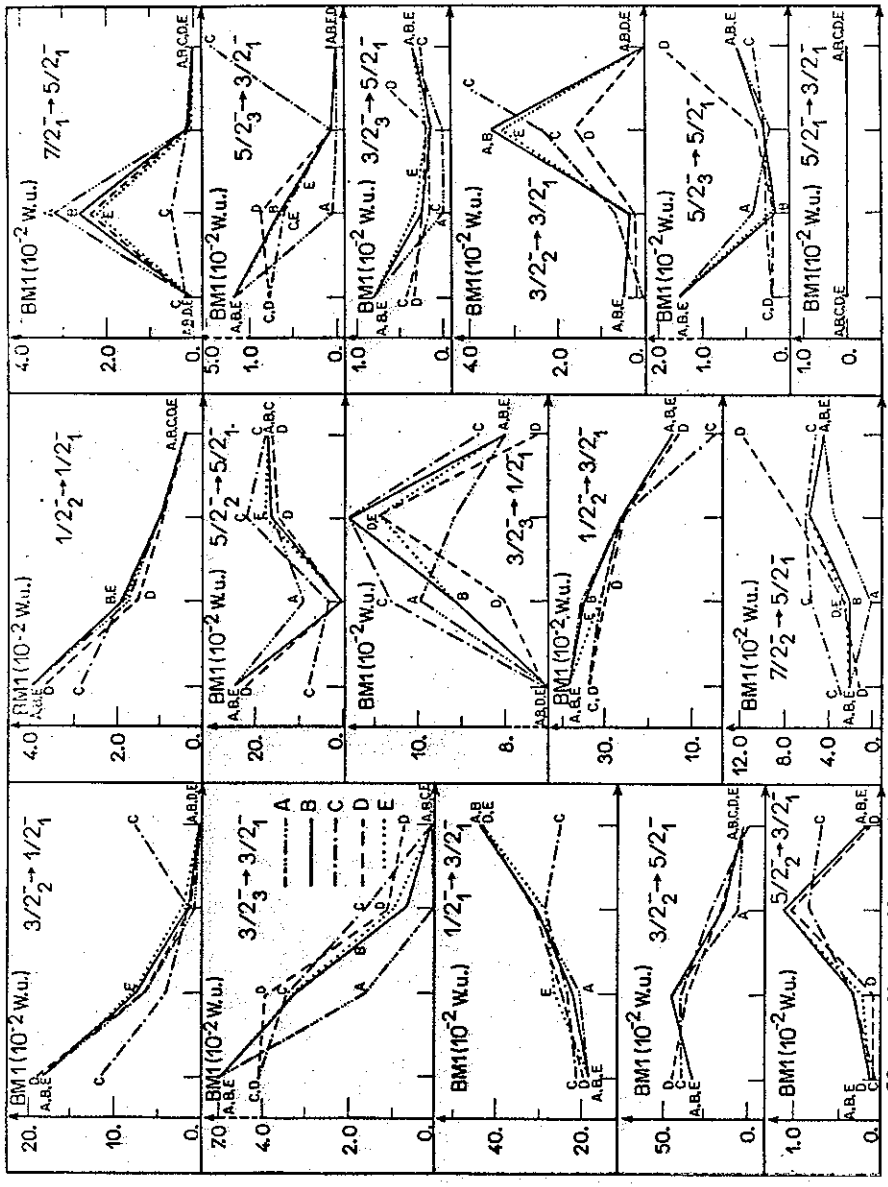
BM1(10⁻² W.u.)
7/2₁⁻ → 5/2₁⁻
5/2₃⁻ → 3/2₁⁻
3/2₃⁻ → 5/2₁⁻
3/2₂⁻ → 3/2₁⁻
5/2₃⁻ → 5/2₁⁻
5/2₁⁻ → 3/2₁⁻
1/2₂⁻ → 1/2₁⁻
5/2₂⁻ → 5/2₁⁻
3/2₃⁻ → 1/2₁⁻
1/2₂⁻ → 3/2₁⁻
7/2₂⁻ → 5/2₁⁻
3/2₂⁻ → 1/2₁⁻
3/2₃⁻ → 3/2₁⁻
1/2₁⁻ → 3/2₁⁻
3/2₂⁻ → 5/2₁⁻
5/2₂⁻ → 3/2₁⁻
A
B
C
D
E

Fig. 12

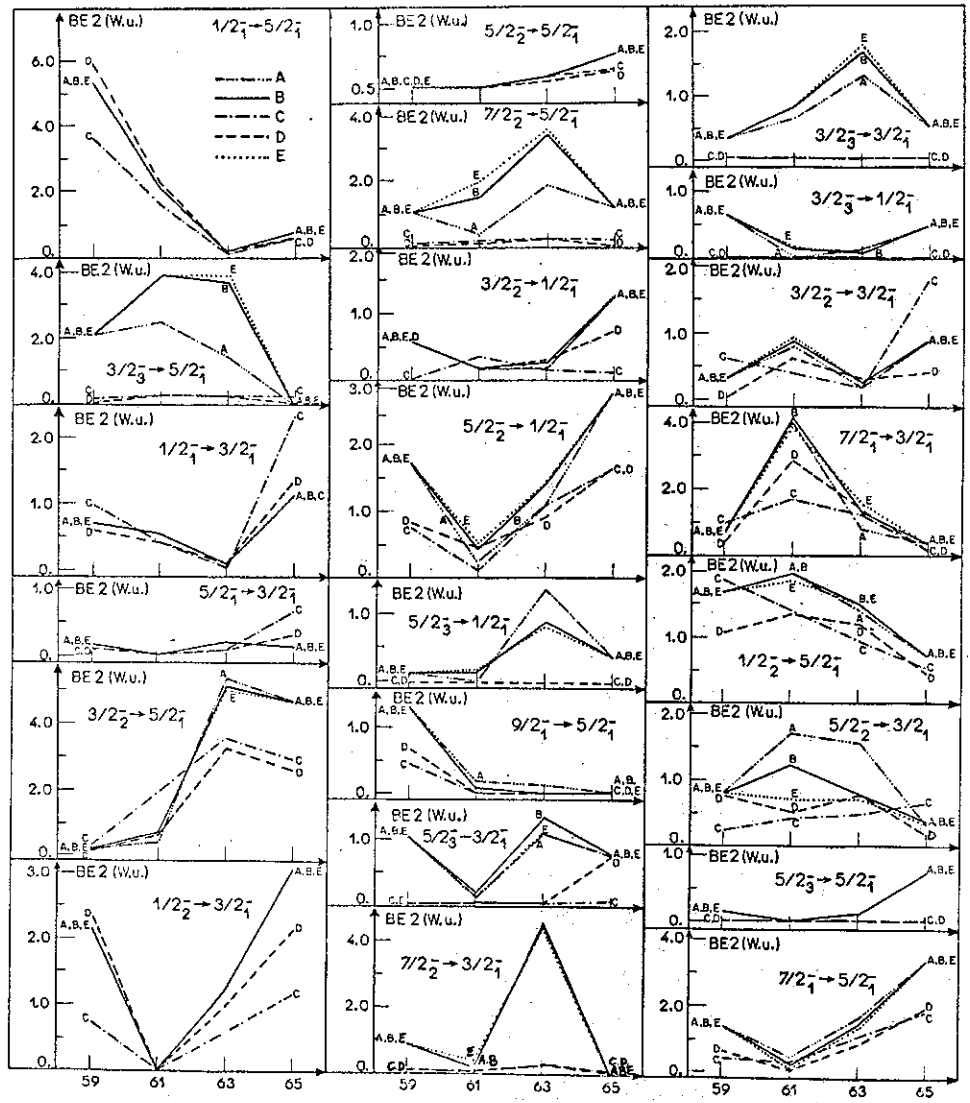
BE 2 (W.u.)
1/2₁⁻ → 5/2₁⁻
5/2₂⁻ → 5/2₁⁻
3/2₃⁻ → 3/2₁⁻
7/2₂⁻ → 5/2₁⁻
3/2₃⁻ → 1/2₁⁻
3/2₃⁻ → 5/2₁⁻
3/2₂⁻ → 1/2₁⁻
3/2₂⁻ → 3/2₁⁻
1/2₁⁻ → 3/2₁⁻
5/2₂⁻ → 1/2₁⁻
7/2₁⁻ → 3/2₁⁻
5/2₁⁻ → 3/2₁⁻
1/2₂⁻ → 5/2₁⁻
3/2₂⁻ → 5/2₁⁻
5/2₃⁻ → 1/2₁⁻
9/2₁⁻ → 5/2₁⁻
5/2₂⁻ → 3/2₁⁻
5/2₃⁻ → 3/2₁⁻
5/2₃⁻ → 5/2₁⁻
1/2₂⁻ → 3/2₁⁻
7/2₂⁻ → 3/2₁⁻
7/2₁⁻ → 5/2₁⁻
A
B
C
D
E

Fig. 13

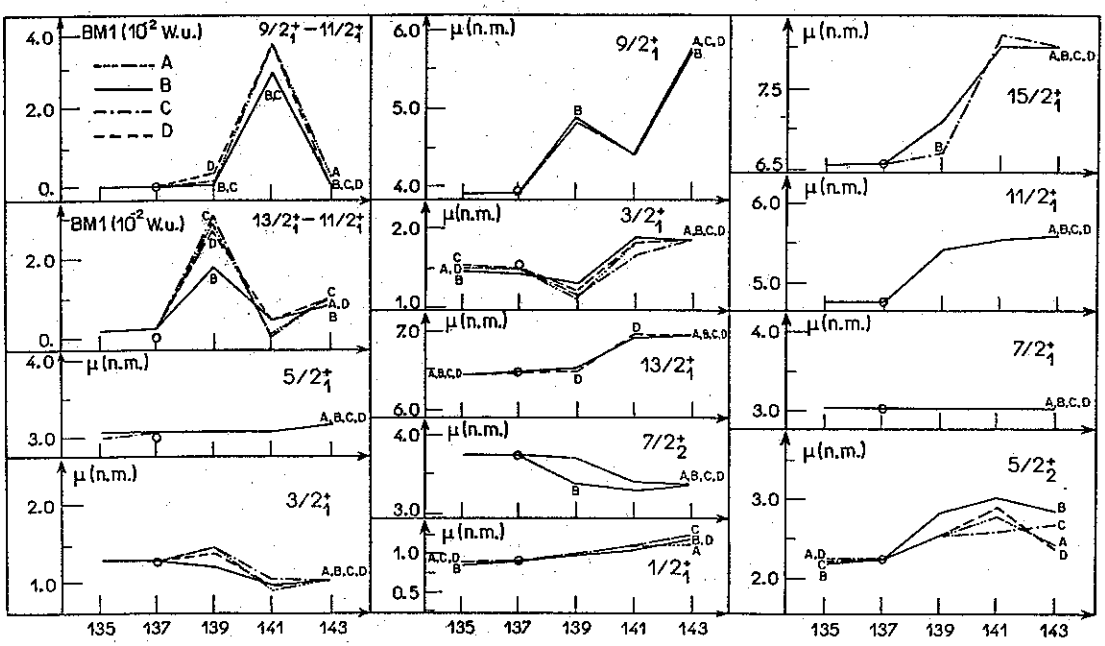
BM1 (10^2 W.u.)
$9/2_1^+ - 11/2_1^+$
A
B
C
D
$13/2_1^+ - 11/2_1^+$
μ (n.m.)
$5/2_1^+$
$3/2_1^+$
$9/2_1^+$
$3/2_1^+$
$13/2_1^+$
$7/2_2^+$
$1/2_1^+$
$15/2_1^+$
$11/2_1^+$
$7/2_1^+$
$5/2_2^+$
135 137 139 141 143

Fig. 14

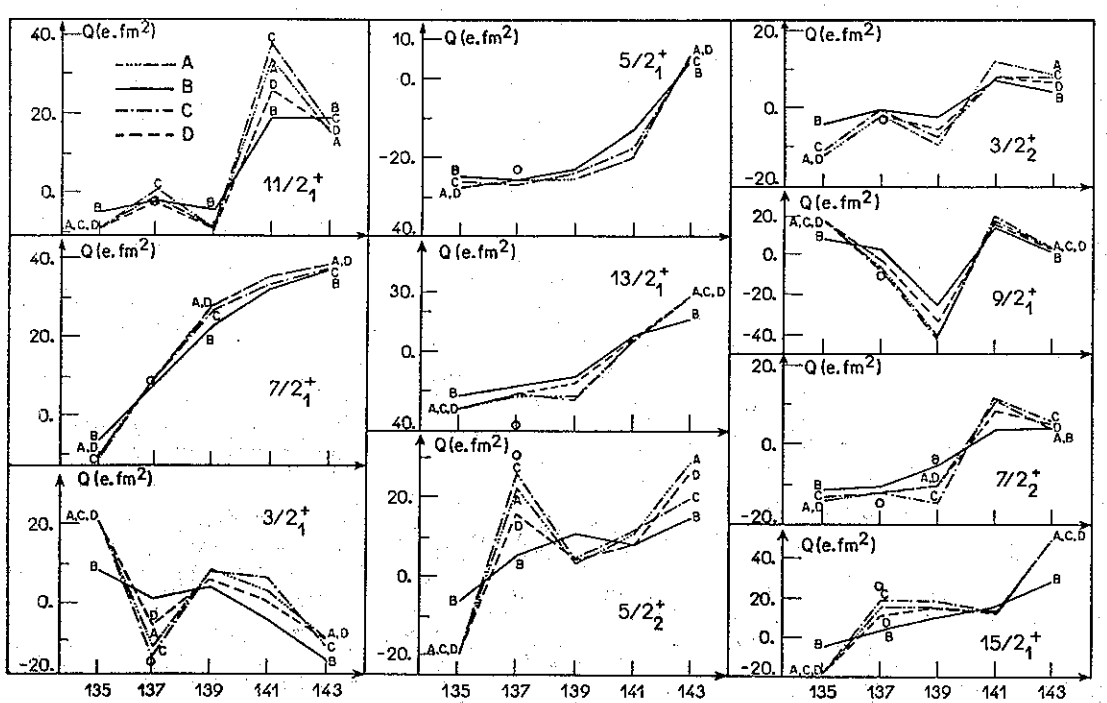
Q (e.fm^2)
A
B
C
D
$11/2_1^+$
$7/2_1^+$
$3/2_1^+$
$5/2_1^+$
$13/2_1^+$
$5/2_2^+$
$3/2_2^+$
$9/2_1^+$
$7/2_2^+$
$15/2_1^+$
135 137 139 141 143

Fig. 15

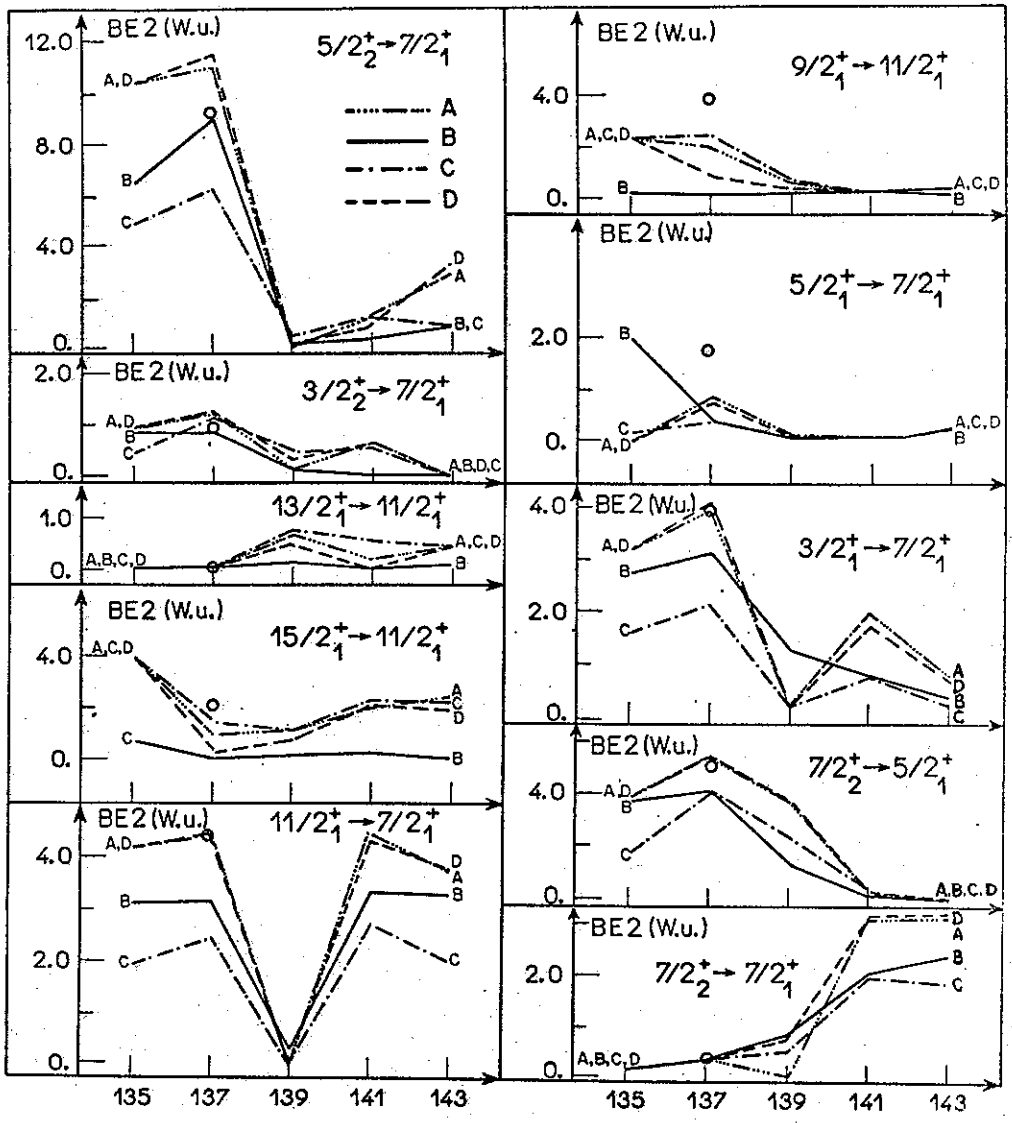
BE2 (W.u.)
$5/2_2^+ \rightarrow 7/2_1^+$
A
B
C
D
$9/2_1^+ \rightarrow 11/2_1^+$
$5/2_1^+ \rightarrow 7/2_1^+$
$3/2_2^+ \rightarrow 7/2_1^+$
$13/2_1^+ \rightarrow 11/2_1^+$
$3/2_1^+ \rightarrow 7/2_1^+$
$15/2_1^+ \rightarrow 11/2_1^+$
$7/2_2^+ \rightarrow 5/2_1^+$
$11/2_1^+ \rightarrow 7/2_1^+$
$7/2_2^+ \rightarrow 7/2_1^+$
135
137
139
141
143

Fig. 16

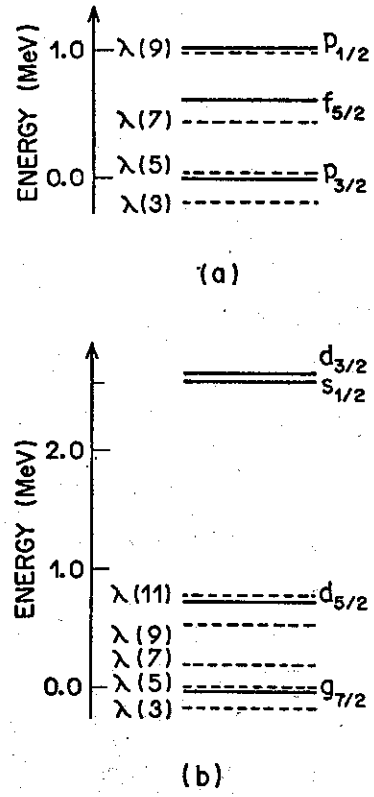
ENERGY (MeV)
1.0
0.0
λ(9)
λ(7)
λ(5)
λ(3)
$p_{1/2}$
$f_{5/2}$
$p_{3/2}$
(a)
2.0
1.0
0.0
λ(11)
λ(9)
λ(7)
λ(5)
λ(3)
$d_{3/2}$
$s_{1/2}$
$d_{5/2}$
$g_{7/2}$
(b)

Fig. 17